A lower density universe?

Measuring imprints of large scale structure on the CMB

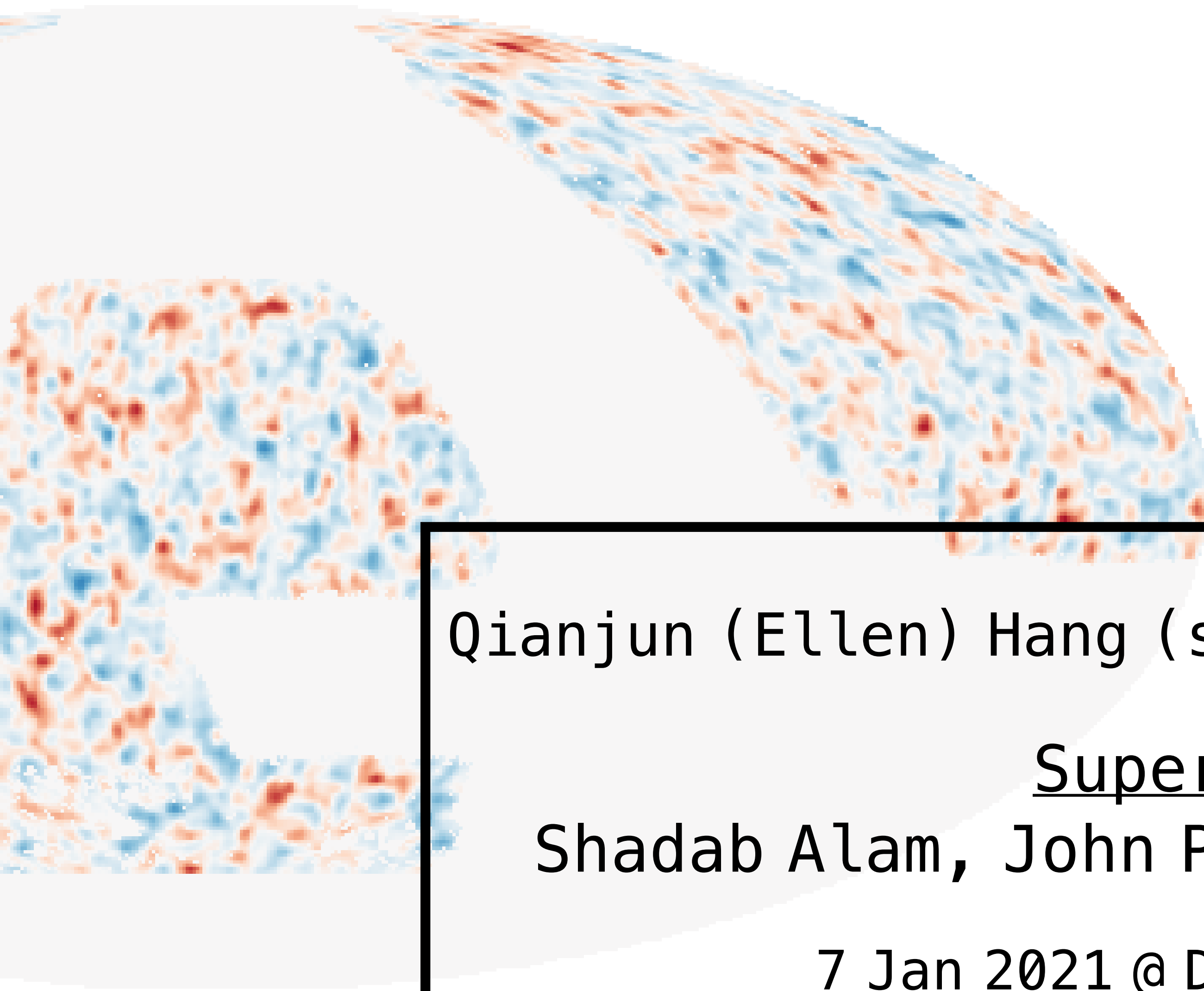

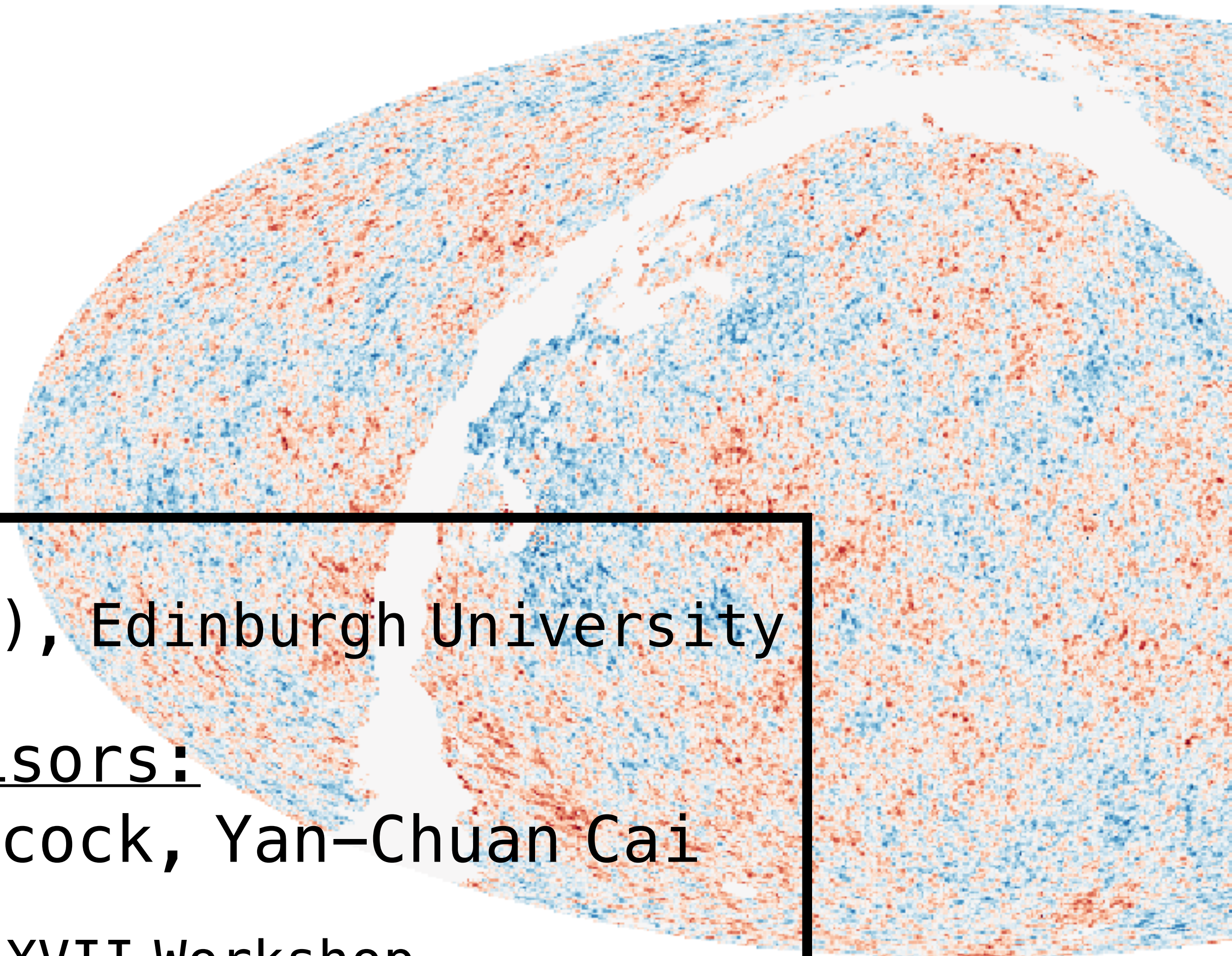

Qianjun (Ellen) Hang (she), Edinburgh University

<u>Supervisors:</u>
Shadab Alam, John Peacock, Yan-Chuan Cai

7 Jan 2021 @ DEX XVII Workshop

European Research Council
Established by the European Commission

Q. Hang et al 2020, MNRAS [2010.00466]

https://www.esa.int/Science_Exploration/Space_Science/Planck/History_of_cosmic_structure_formation

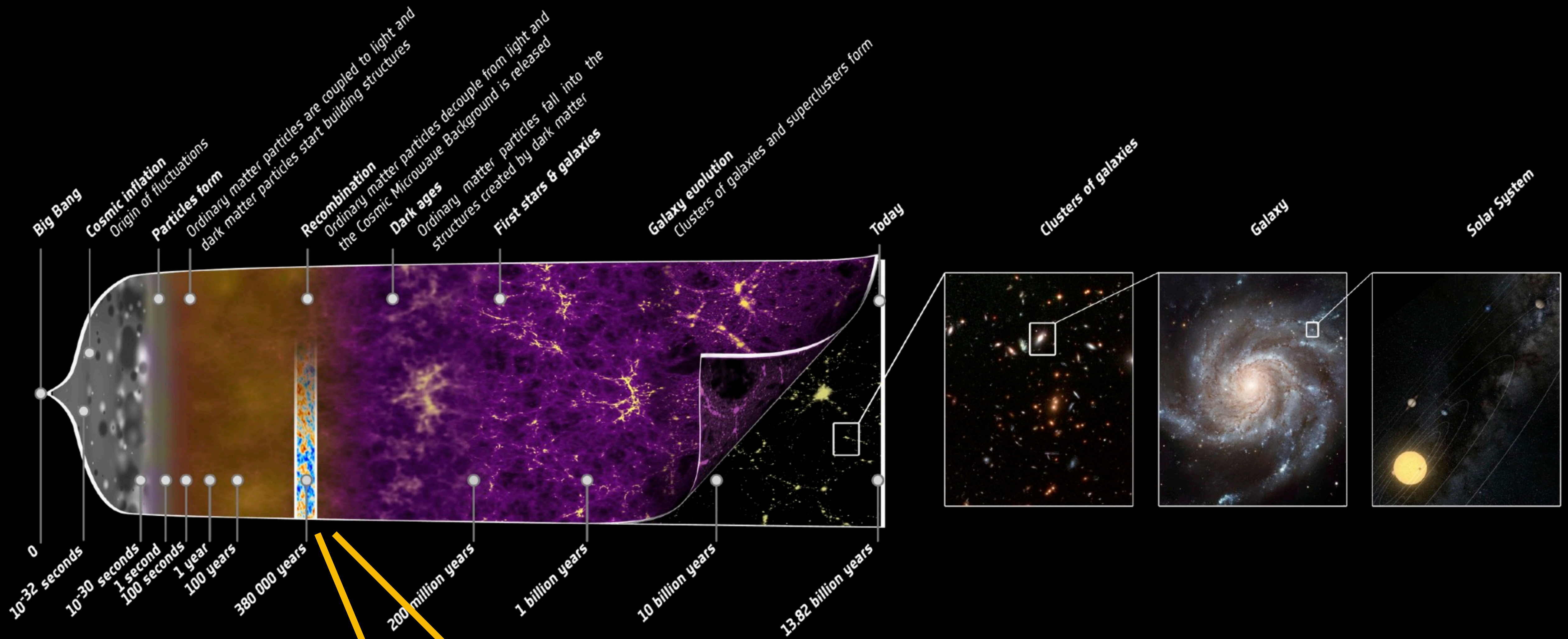

CMB temperature

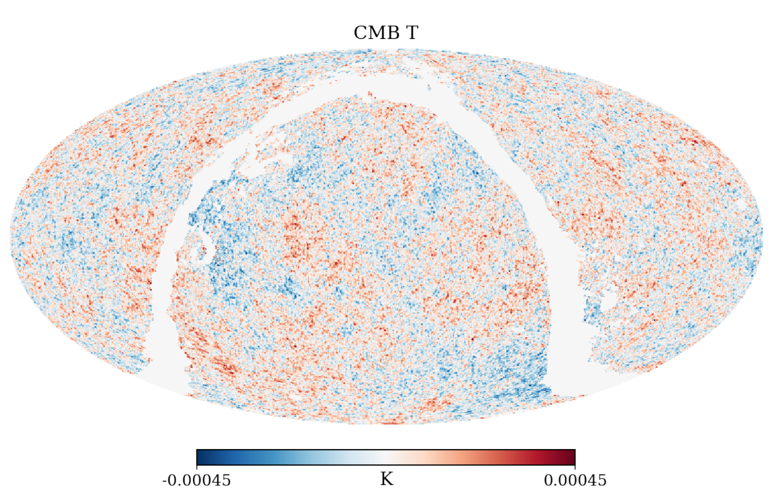

CMB lensing convergence

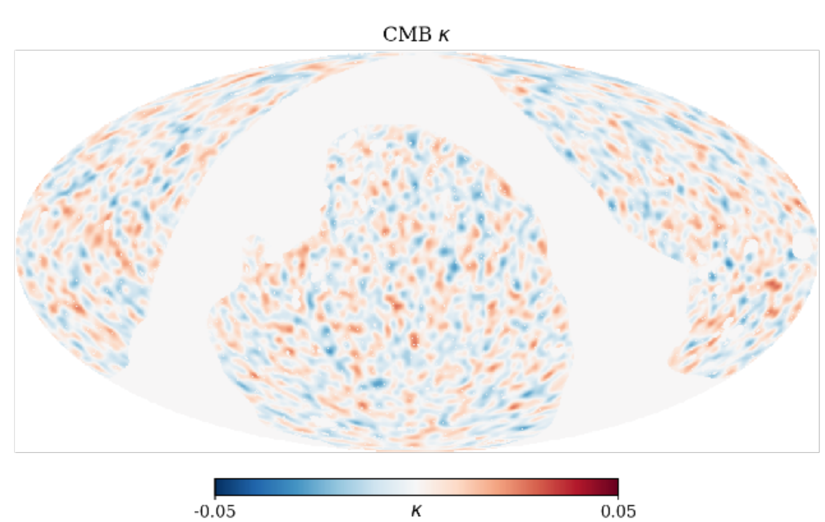

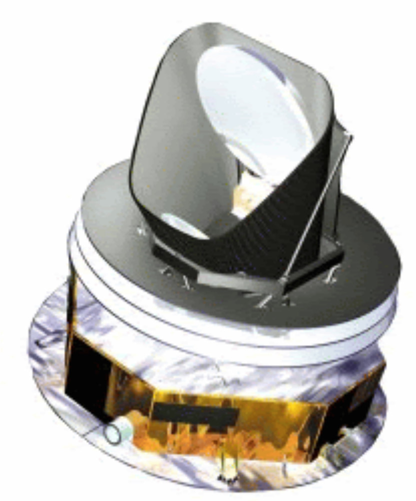

Integrated Sachs–Wolfe (ISW) effect

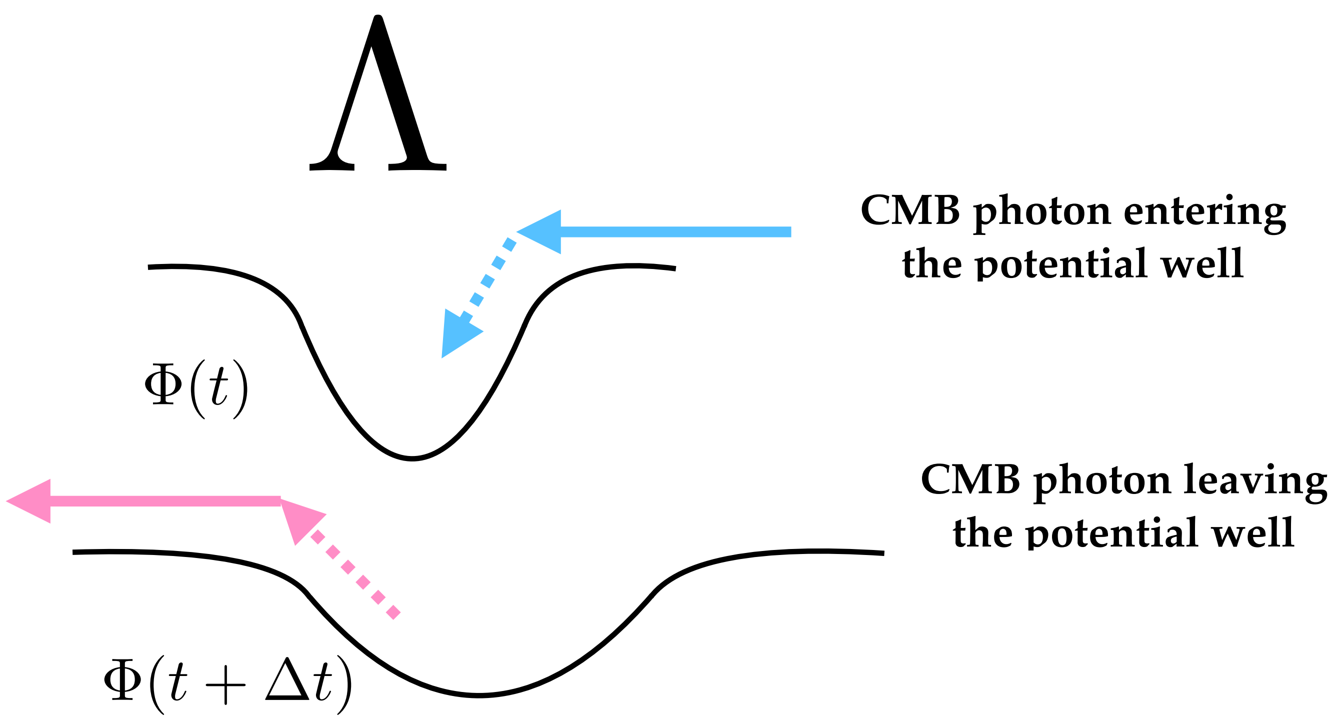

$$\frac{\Delta T}{T} = -\frac{2}{c^2}\int \dot{\Phi}\, dt$$

Photon frequency modified

↓

The CMB temperature fluctuations are modulated

Gravitational lensing

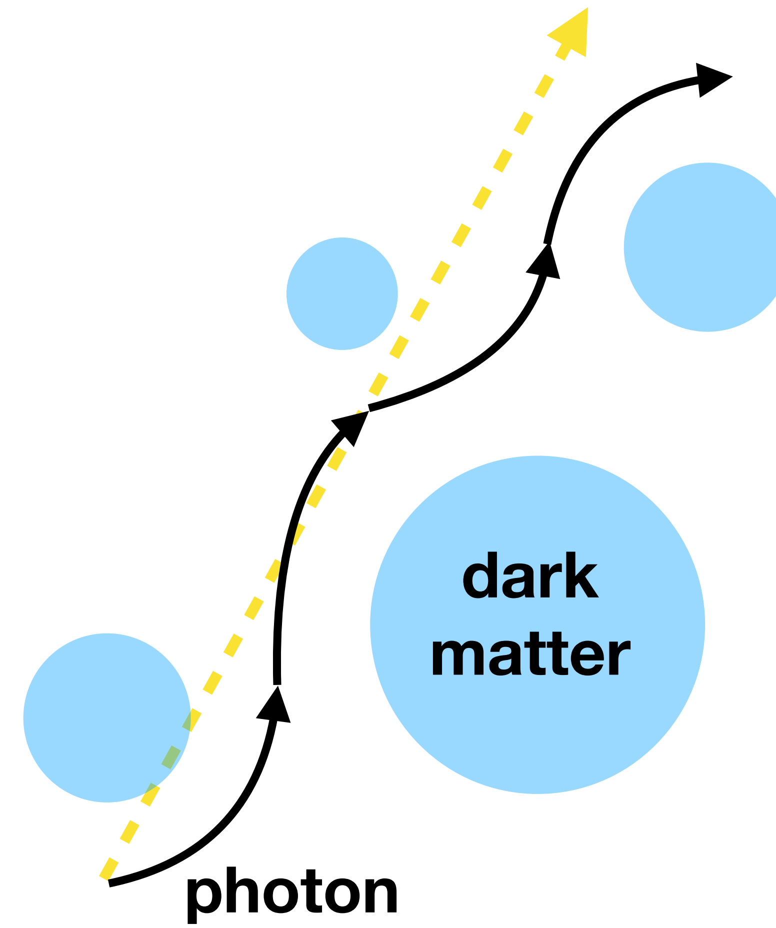

$$\kappa = \frac{1}{2}\nabla^2\psi$$

Photon trajectory modified

↓

Results in CMB lensing convergence.

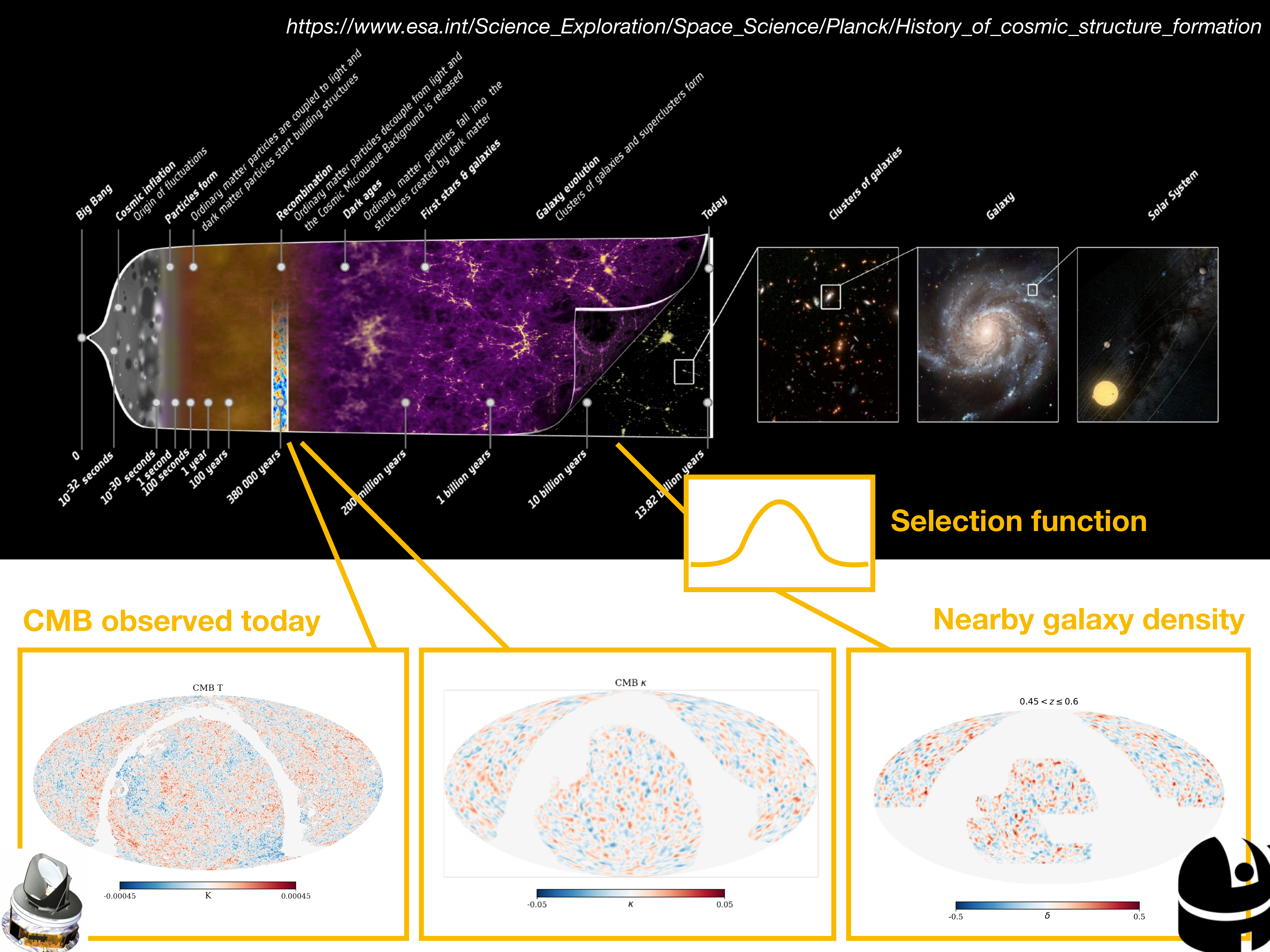

https://www.esa.int/Science_Exploration/Space_Science/Planck/History_of_cosmic_structure_formation
Big Bang
Cosmic inflation
Origin of fluctuations
Particles form
Ordinary matter particles are coupled to light and dark matter particles start building structures
Recombination
Ordinary matter particles decouple from light and the Cosmic Microwave Background is released
Dark ages
Ordinary matter particles fall into the structures created by dark matter
First stars & galaxies
Galaxy evolution
Clusters of galaxies and superclusters form
Today
Clusters of galaxies
Galaxy
Solar System
0
10-32 seconds
10-30 seconds
1 second
100 seconds
1 year
100 years
380 000 years
200 million years
1 billion years
10 billion years
13.82 billion years
Selection function
CMB observed today
Nearby galaxy density
CMB T
-0.00045
K
0.00045
CMB κ
-0.05
κ
0.05
0.45 < z ≤ 0.6
-0.5
δ
0.5

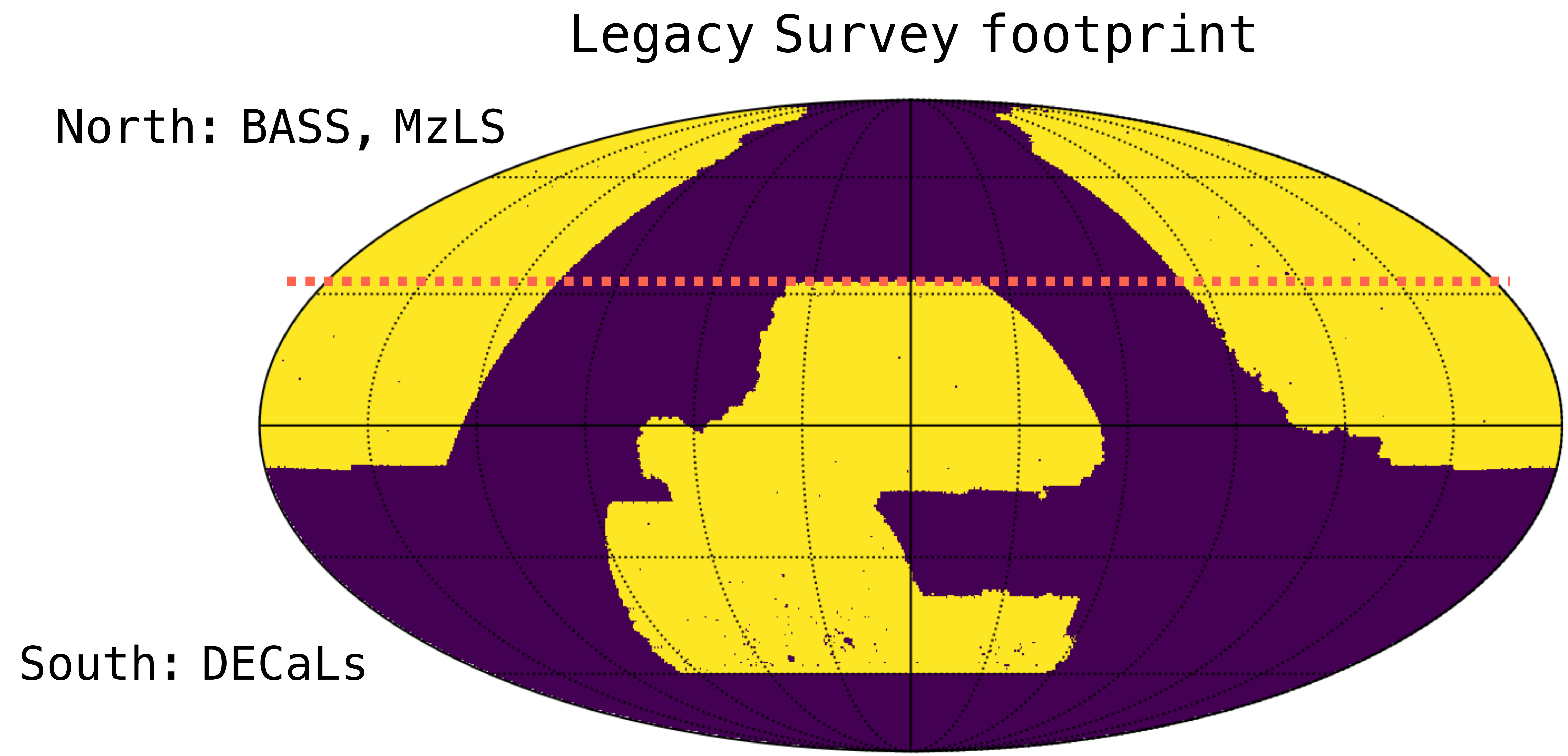

- The Public DESI Legacy Imaging Survey (DR7)
- 14,000 deg^2, about 1/3 of the whole sky
- Depth: g=24, r=23.4, z=22.5 (optical wavelength), matched WISE bands: W1, W2, W3 (infrared wavelength)

Calibration of the photometric redshifts

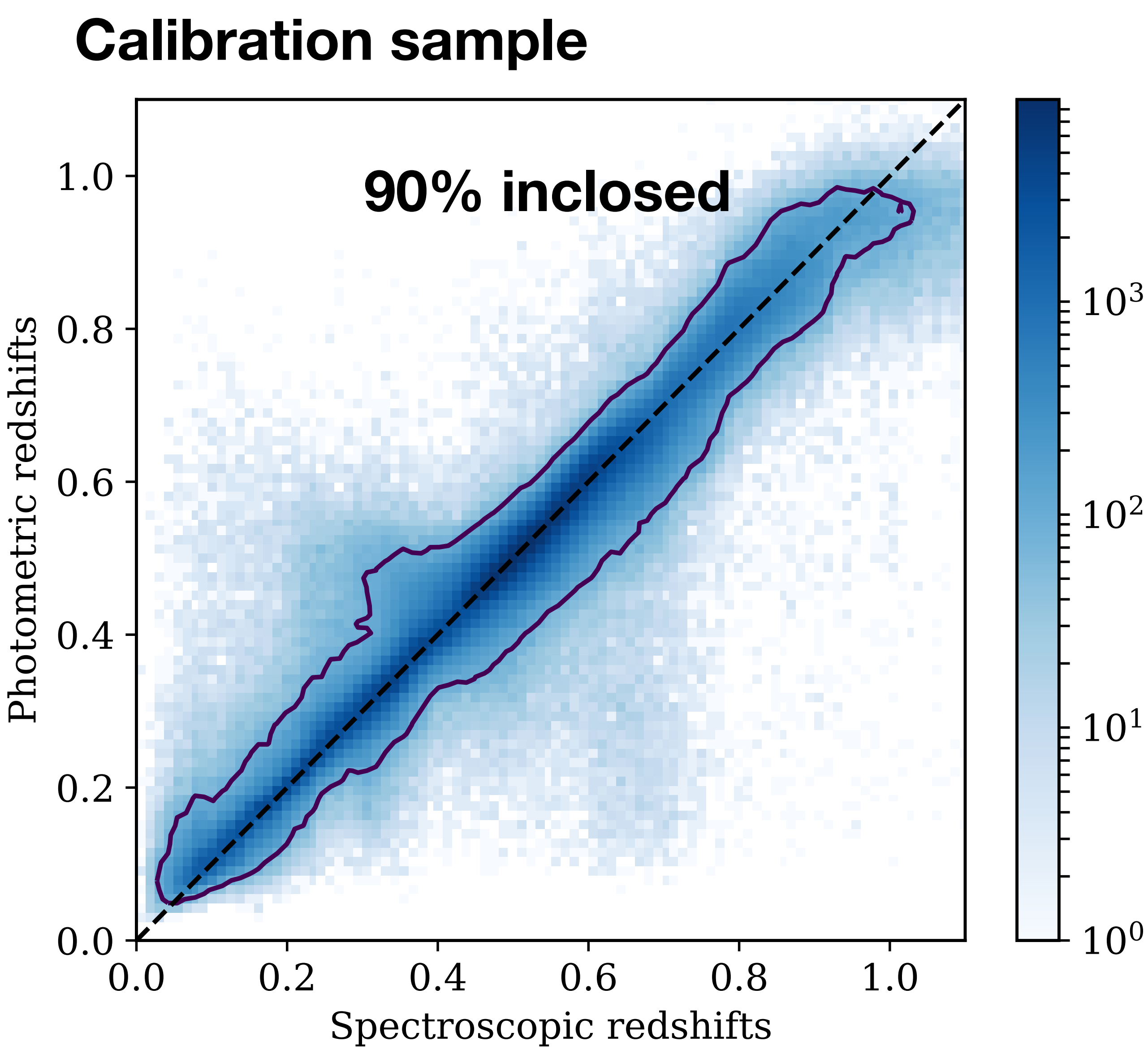

- Calibration with spectroscopic samples
- 3D colour grids: g−r, r−z, z−W1, with pixel width of ~0.03mag.
- Galaxies falling outside the grid covered by the calibration sample are excluded
- 78.6% of the selected Legacy Survey galaxies assigned photometric redshift

Photo-z uncertainties and galaxy bias

- 4 tomographic bins with 0<z<0.8
- 7 photo-z parameters in total, fitted by galaxy cross-correlation between different redshift bins

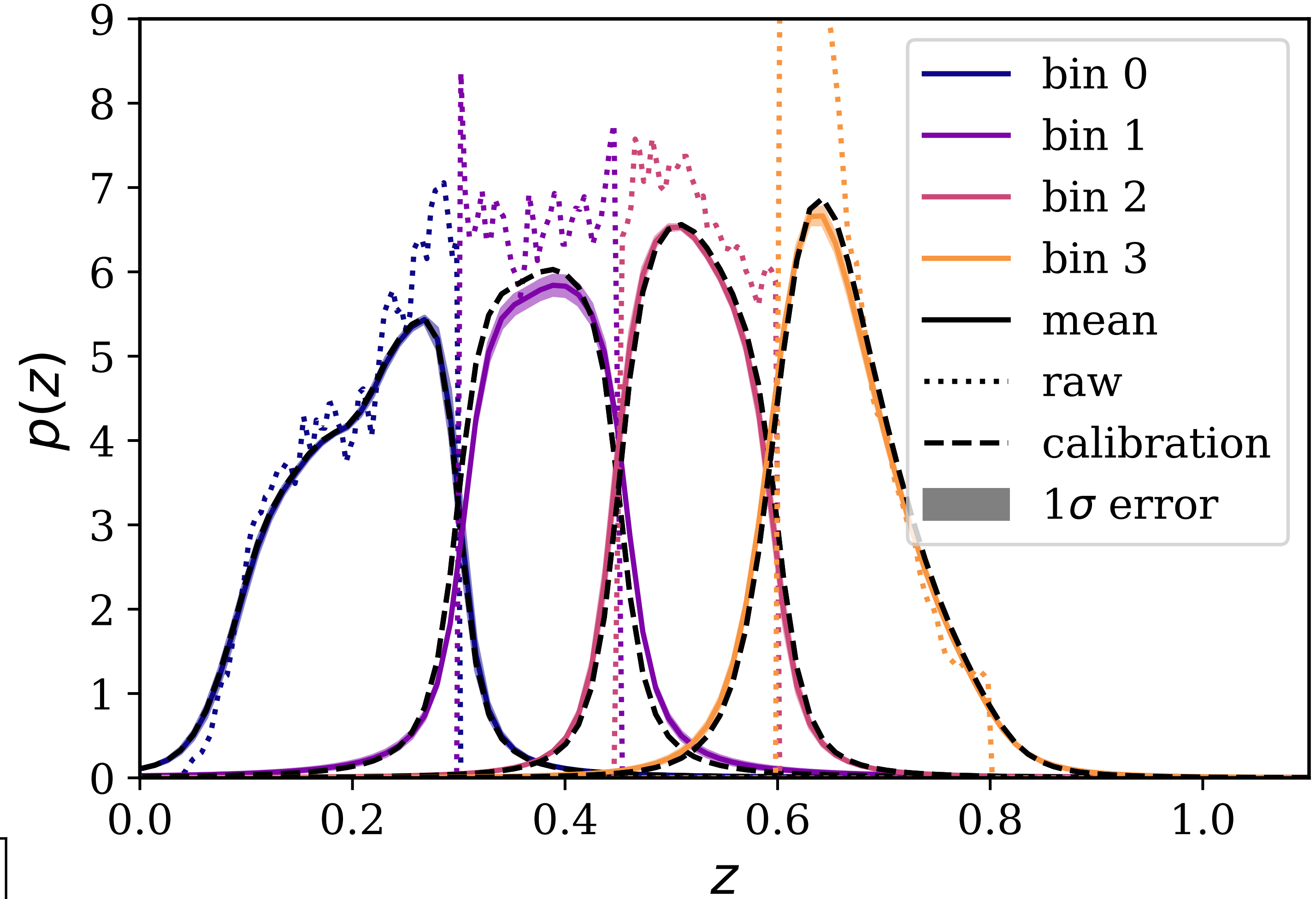

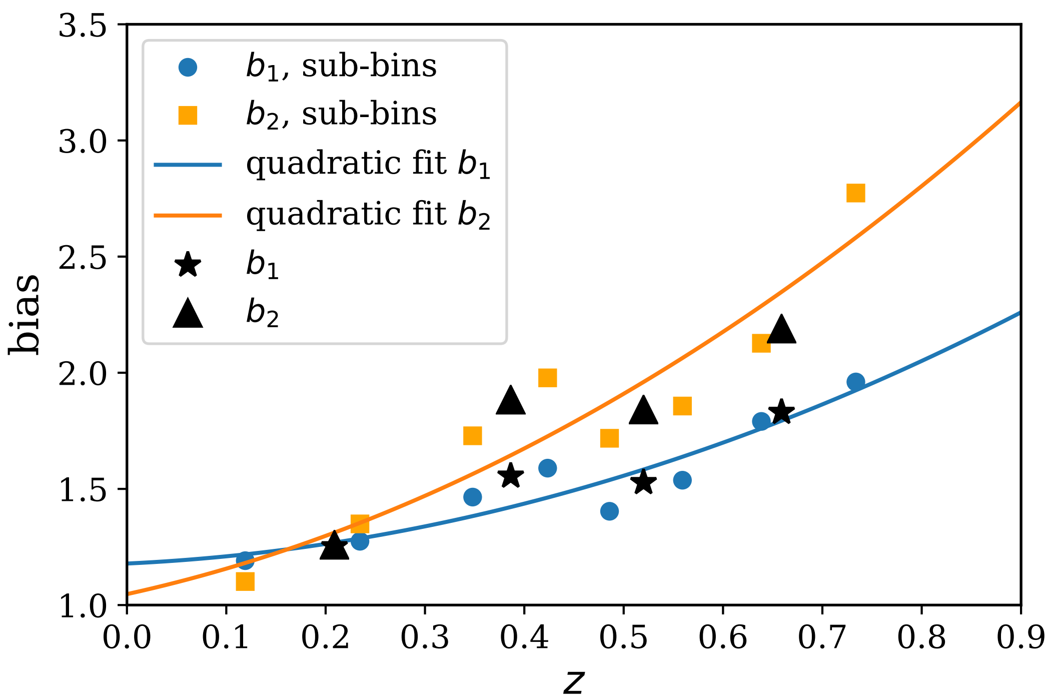

- The galaxy biases (and the evolution) are fixed from galaxy auto-correlations
- p(z) and bias are fixed for cross-correlation analysis

Galaxy density maps

Final selection has ~4.5x10^7 galaxies

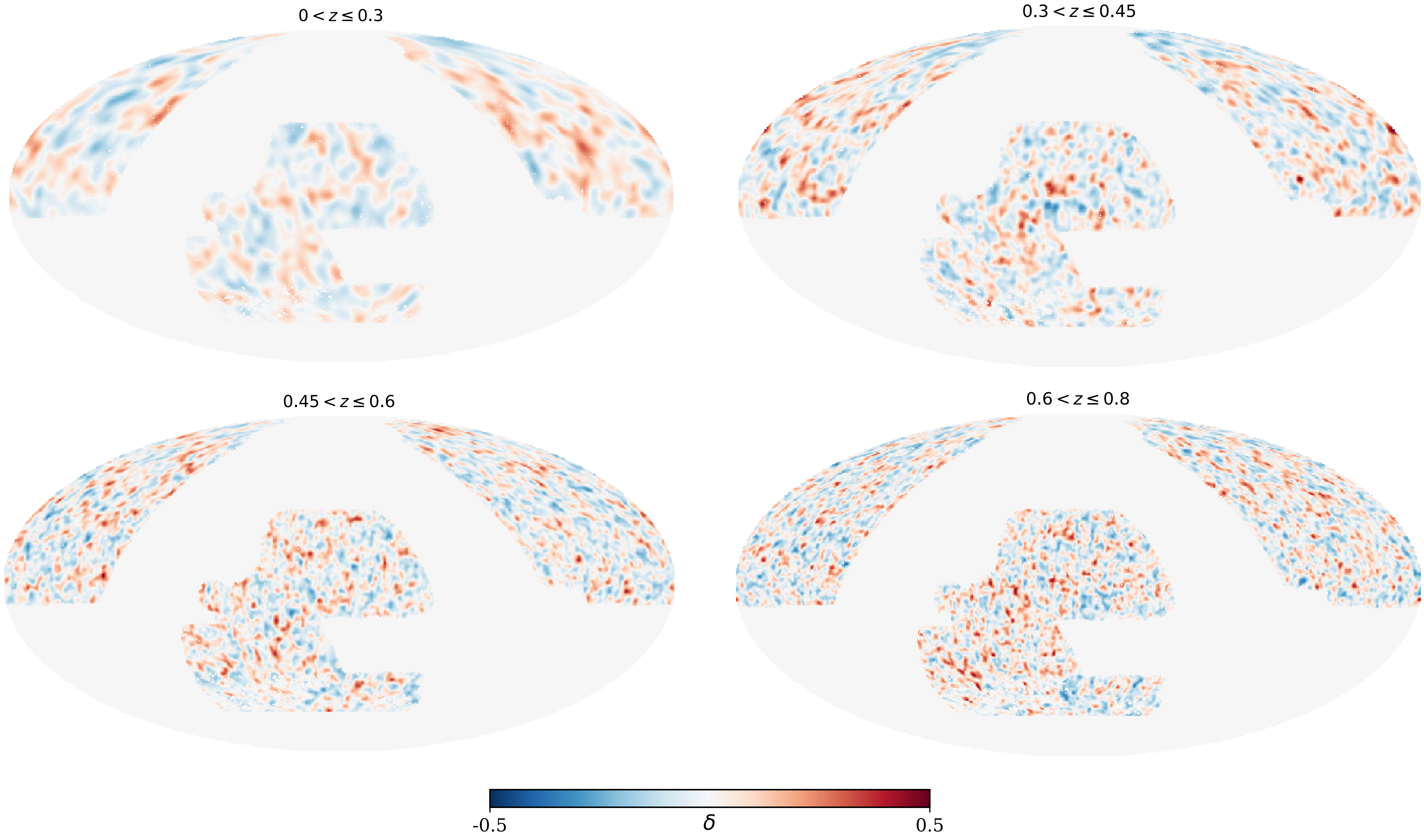

Results

Cross-correlations with the CMB maps – ISW results

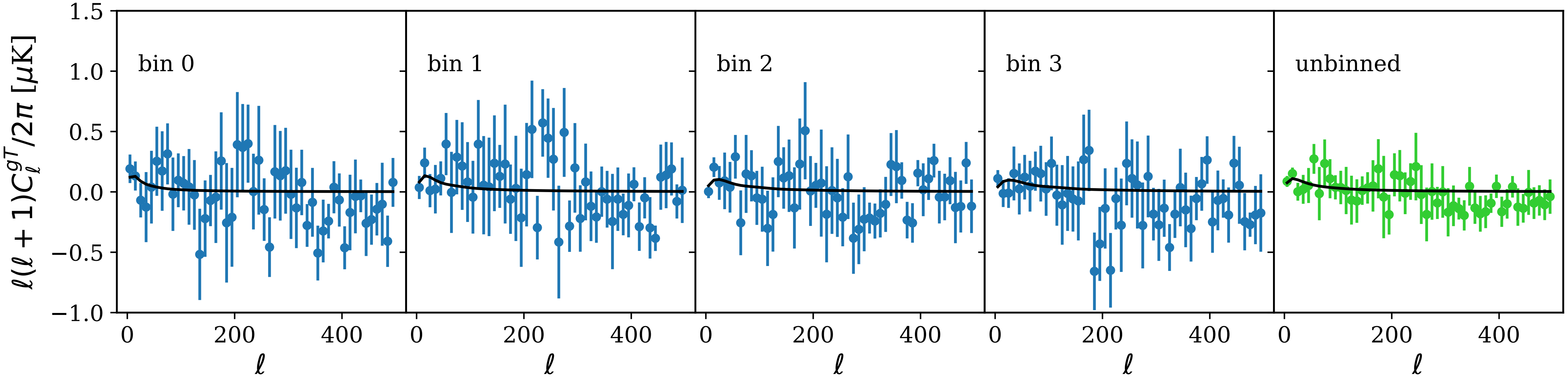

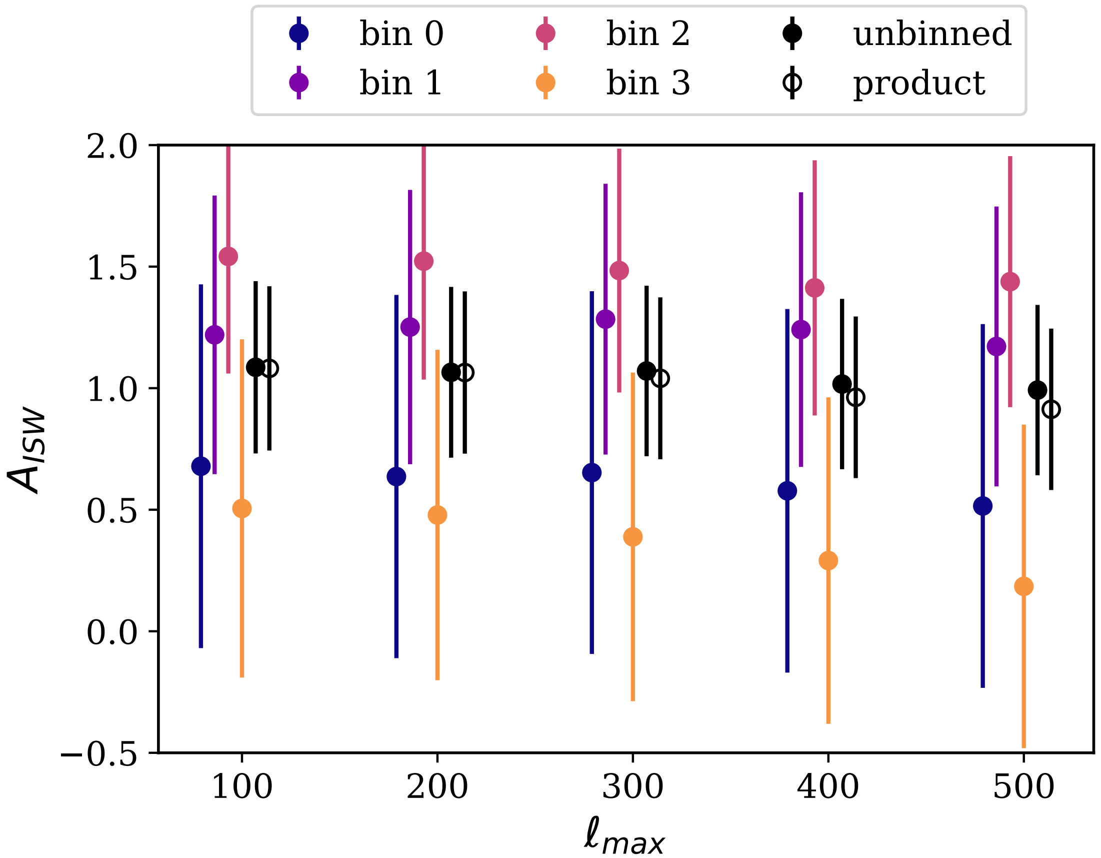

- The ISW signal is very noisy.
- We find that $A_{\rm ISW} = 0.98 \pm 0.35$
- It is fully consistent with the fiducial cosmology given the large error bar.

Cross-correlations with the CMB maps – lensing results

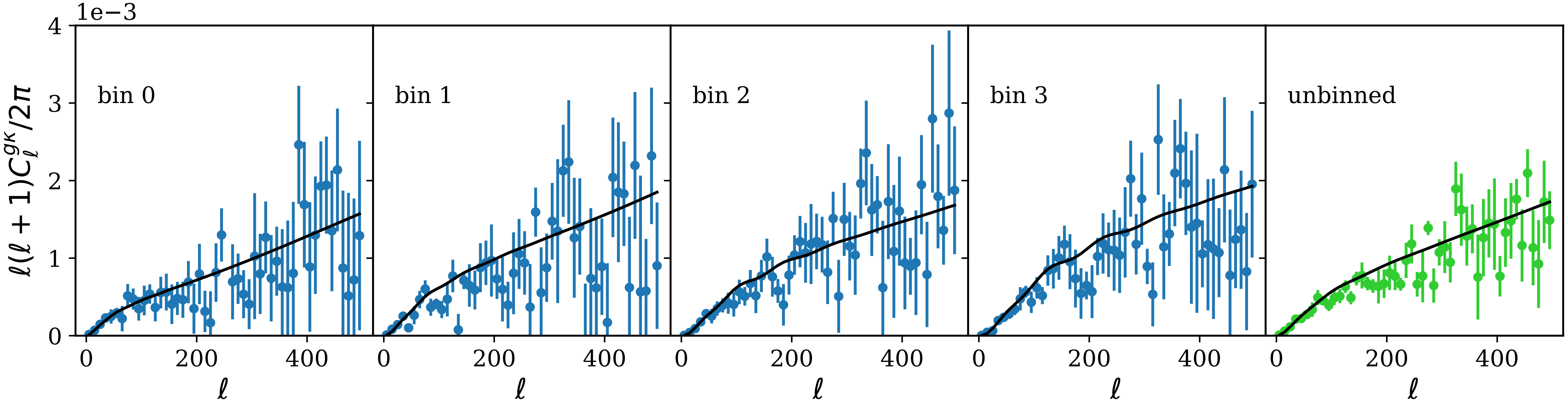

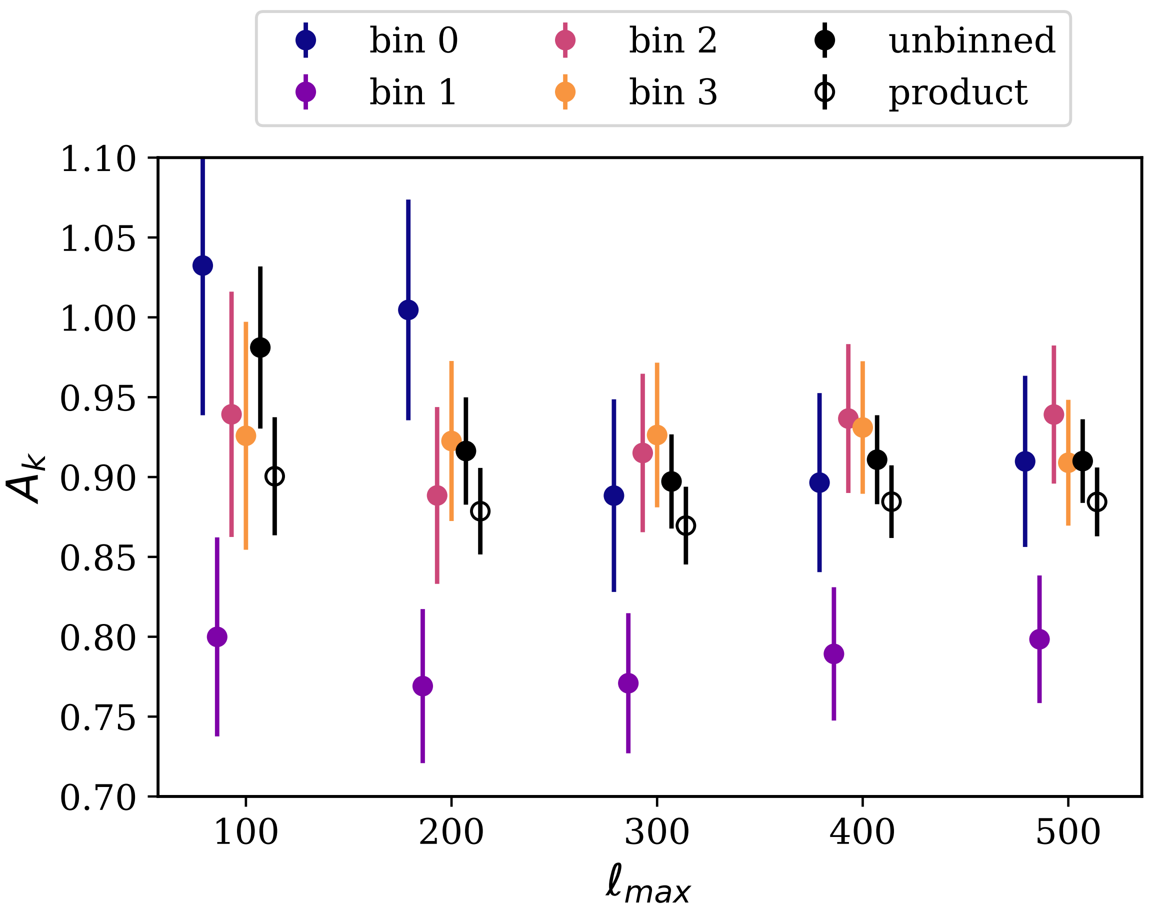

The result of combining the four redshift bins and the un-binned case consistently lie below unity.

$$A_\kappa = 0.901 \pm 0.026$$

The lensing signal

$$\frac{\ell(\ell+1)}{2\pi} C_\ell^{gX} = \frac{\pi}{\ell} \int b\,\Delta^2(k=\ell/r, z)\,p(z) K^X(z) r\,dz$$

X=lensing $$K^\kappa = \frac{3H_0^2\Omega_m}{2c^2 a} \frac{r(r_{\rm LS}-r)}{r_{\rm LS}}$$

$b\sigma_8$ fixed by auto-correlation,

At z=0, the signal is directly proportional to $\sigma_8\Omega_m$.

At z~0.5, we verify that the dependence is $A_k \propto \sigma_8\Omega_m^{0.78}$.

Cosmological implications of low A_κ

Fiducial: Planck 2018 best-fit parameters

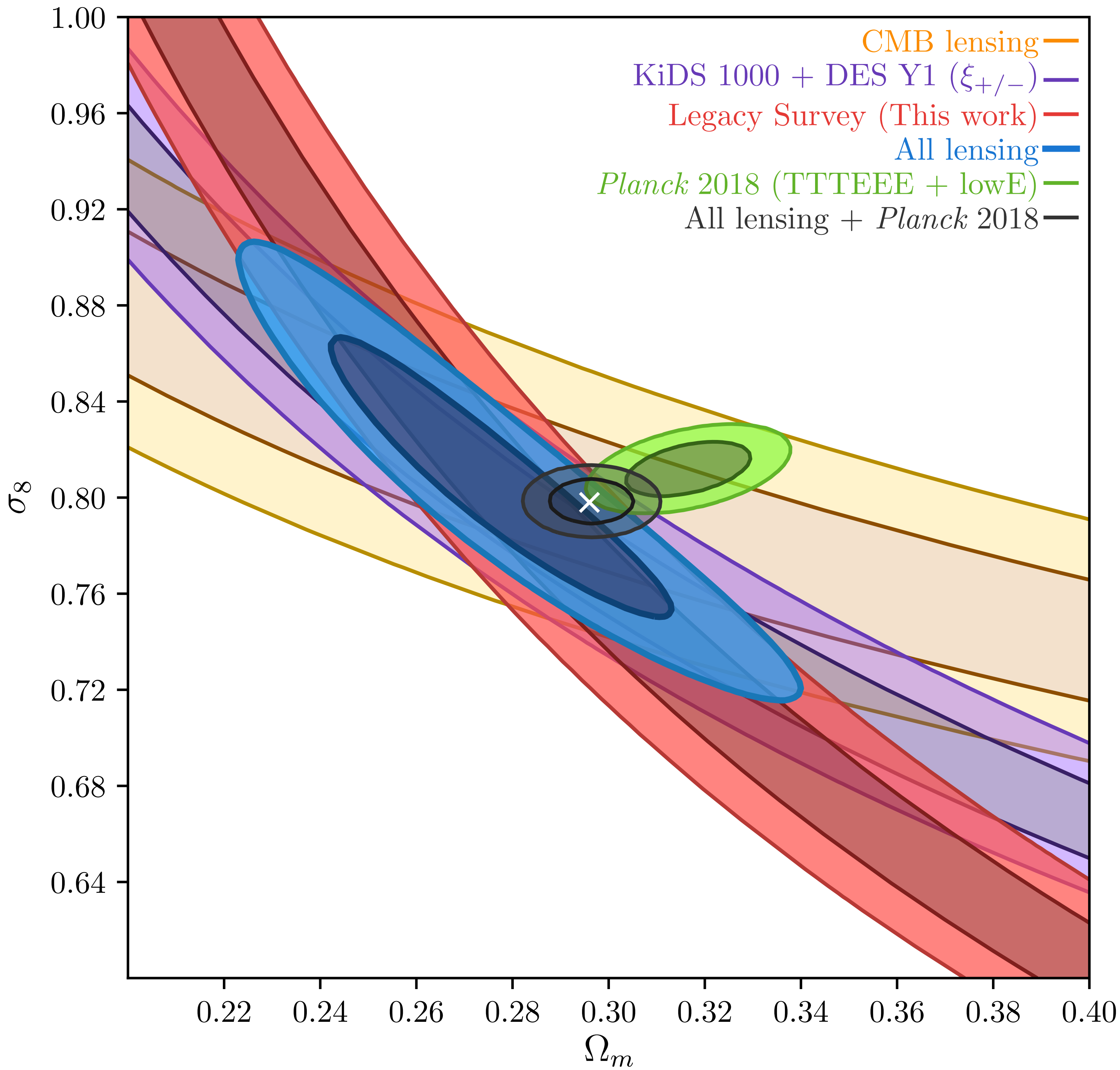

$$\Omega_m = 0.315 \quad \sigma_8 = 0.811$$

Our results put a constraint on the quantity: $\sigma_8\Omega_m^{0.78}=0.297\pm0.009$.

Combined with total CMB lensing, we prefer a lower matter density:

$$\Omega_m = 0.275 \pm 0.024$$
$$\sigma_8 = 0.814 \pm 0.042$$

A lower density universe?

- Bad luck with statistics?
- Systematics in galaxy data, e.g., photo-z, contamination, magnification bias…
- Planck internal inconsistency?
- Modelling? [Kitanidis & White, 2020] found similar results with LRG using halofit, but not in perturbation theory.
- Modified gravity? – Theories that modifies the spatial and temporal terms differently maybe be able to achieve lower lensing signal, given the growth rate.

Summary

- We selected galaxies from the DESI Legacy Image Survey and obtained robust photometric redshifts using the available three colour bands.
- We constructed galaxy density maps for four tomographic bins between $0<z<0.8$.
- We measured the cross-correlation between these galaxy maps with the CMB lensing convergence and temperature maps.
- Compared with theoretical prediction based on Planck 2018 Cosmology, we find $A_\kappa=0.901\pm0.026$ and $A_{ISW}=0.98\pm0.35$.
- Our result translate to a strong evidence for lower Ω_m combined other lensing probes.
- Future surveys such as DESI will no doubt provide more insight into this issue!

galaxy-galaxy auto/cross-correlations between redshift slices

$$b$$

- Galaxies are biased tracers of matter, $\delta_g = b\delta_m$
- Constraint by galaxy auto-correlations
- (Data)/(Theory with dark matter)=b^2.

$$p(z)$$

- Photometric redshift distribution is uncertain
- Constraint by galaxy cross-correlations
- Bias independent correlation coefficient:

$$r = \frac{C_\ell^{AB}}{\sqrt{C_\ell^{AA} C_\ell^{BB}}}$$

Methods

- Measurement: Healpy (Healpix) -> pixellated map -> spherical harmonics, a_{lm} -> Angular power spectrum C_l

- Maps: Planck 2018 lensing convergence and temperature maps with masks.

- Theory: non-linear matter power spectrum from CAMB (halofit for the non-linear part)

- Fiducial Cosmology: Planck 2018 best-fit parameters

$$\boxed{\Omega_m = 0.315 \quad \sigma_8 = 0.811} \quad h = 0.674$$

$$n_s = 0.965 \quad \Omega_b = 0.0493$$

2.Legacy Survey and selection

- Exclude PSF types (stars, quasars etc.);
- Require measurements in g, r, z, and w1 bands;
- Apply galactic extinction correction;
- Magnitude cuts: g<24, r<22, w1<19.5 for uniform depth;
- Completeness map from Bitmask: pixels >0.86 -> weights; pixels <0.86 -> masked.
- Normalize North and South separately;
- We correct for stellar density from the ALLWISE total density map (very large scales near galactic plane) more;
- Selection based on 3D colour (see next slide).

~4.5x10^7 galaxies selected

3. Calibration of the photometric redshifts

- Spectroscopic surveys are used to calibrate the redshift of Legacy Survey galaxies (GAMA, BOSS, eBOSS, VIPERS, DEEP2, COSMOS, DESY1A1 redMaGiC). These galaxies are matched in the Legacy Survey sample using their sky positions.

- Mean spec-z in 3D colour grids: g−r, r−z, z−W1, with pixel width of ~0.03mag.

Calibration sample

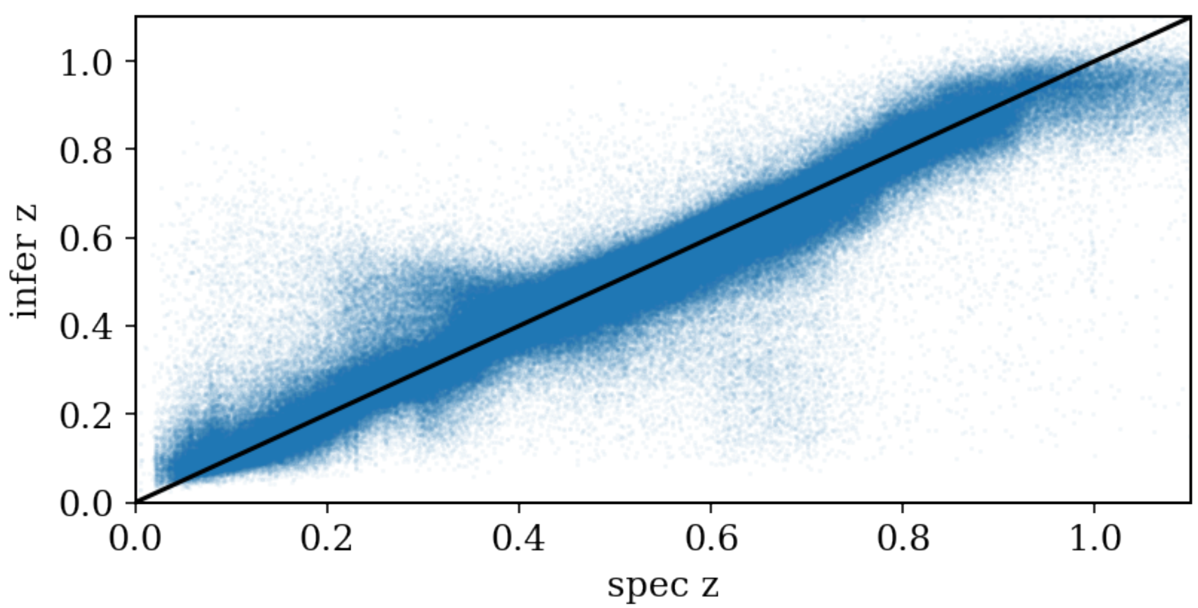

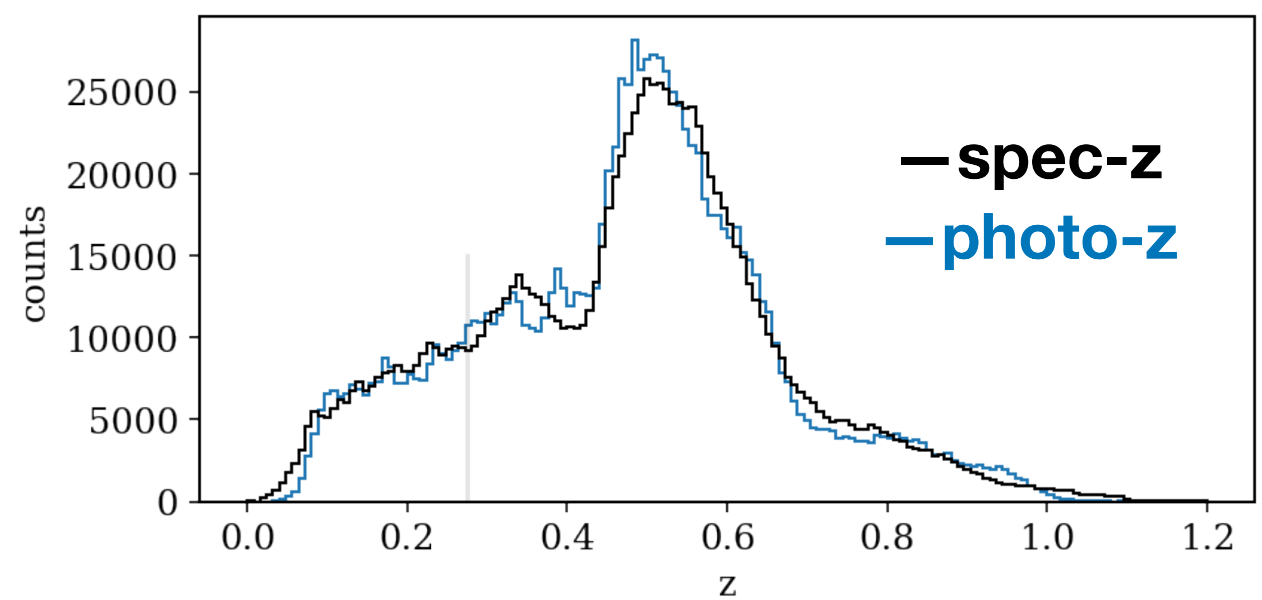

- We assign the mean redshifts in these grids to the Legacy Survey galaxies. Galaxies falling outside the grid covered by the calibration sample are excluded.

- 78.6% of the selected Legacy Survey galaxies get assigned a photometric redshift.

3.Calibration of the photometric redshifts

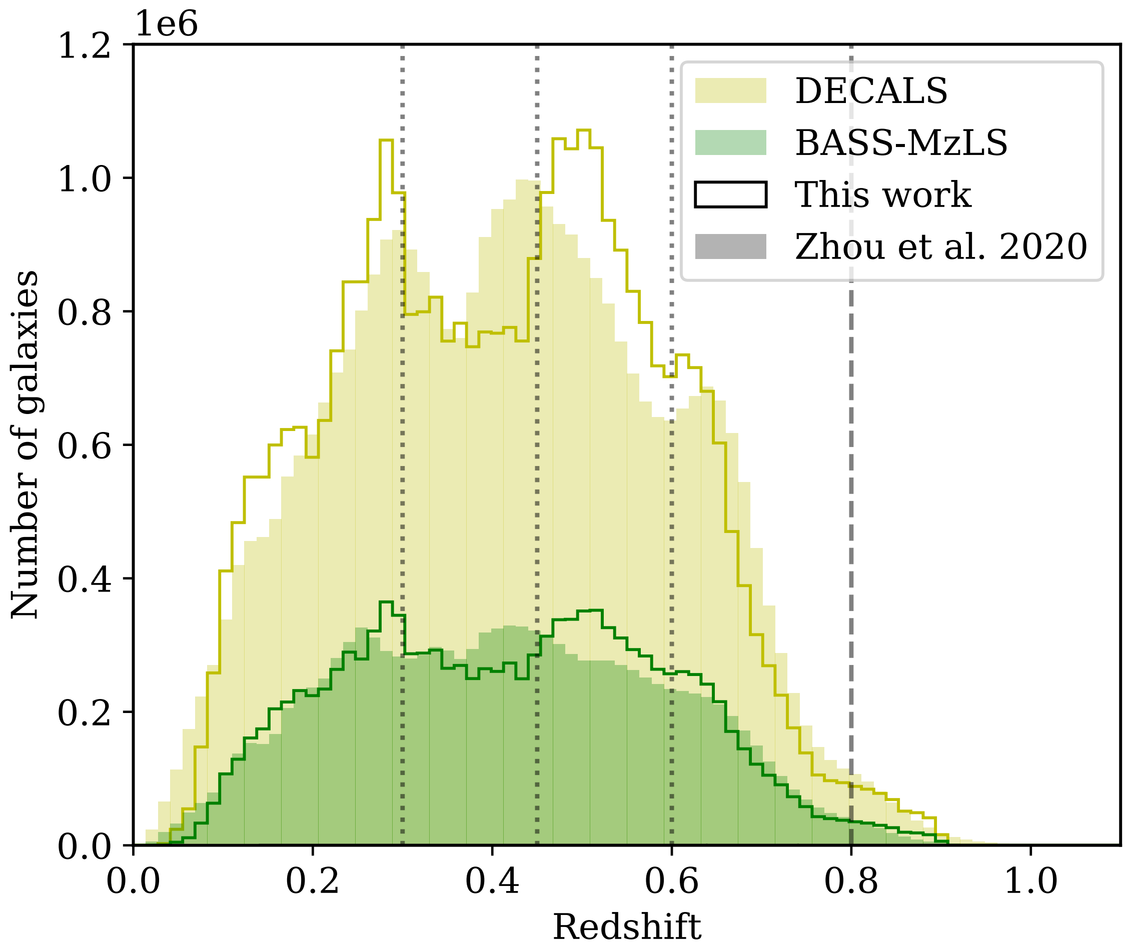

- We also compare with the Zhou et al. (2020) machine-learning photometric redshift catalogue -> select galaxies with |Δz|<0.05.
- We split the sample into 4 tomographic bins in the redshift range 0<z<0.8.

Photo-z error

The raw redshift distribution is convolved with L(x) to obtain the final redshift distribution.

$$L(x) = \frac{N}{(1+((x-x_0)/\sigma)^2/2a)^a}$$

Normalization such that the integral is 1

mean, free with constraint that sum of four bins is zero

width, fixed by fitting the spectroscopic sample in each z bin

Tail, free to account for faint galaxies

4.Cross-correlation Results and errors

- l<10 modes are excluded from fitting.
- We use pseudo-power estimate $\hat{C}_\ell = C_\ell^{\rm masked} / f_{\rm sky}$
- Use Δl=10 power bins. Covariance matrix then accurately diagonal (based on lognormal simulations). more
- Tomographic slices not completely independent. Use un-binned data for combined result.

Galaxy auto-correlations and cross-correlations between different z bins

$$P_g(k) = b_{\rm lin} P_m^{\rm lin}(k) + b_{\rm nl} P_m^{\rm nl}(k)$$

We find that a 2-bias model can fit the data up to l=1000. This model uses separate biases for the linear and non-linear parts of the power spectrum. more

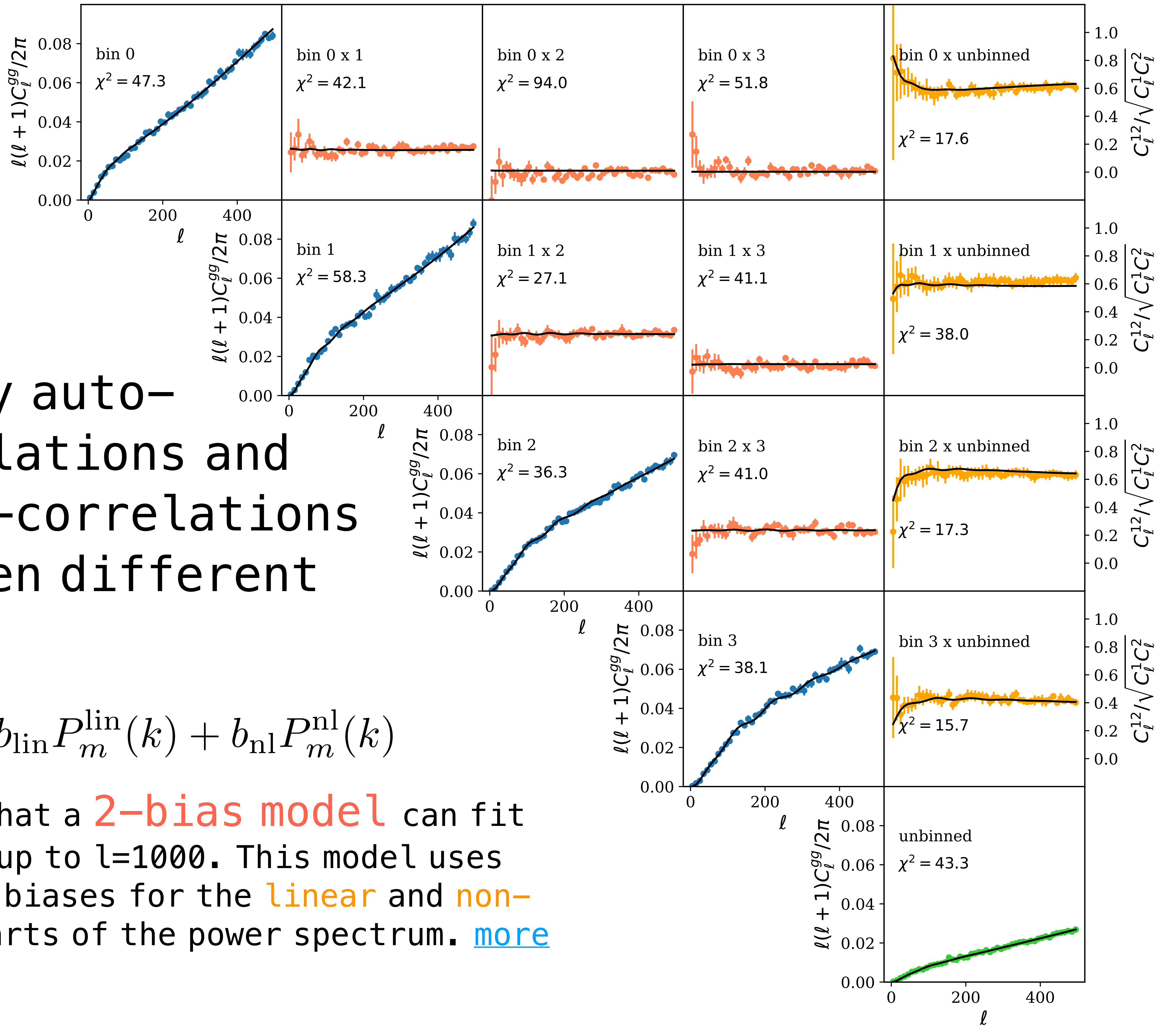

Galaxy auto-correlations and cross-correlations between different z bins

- We minimize the total chi square from the 10 galaxy correlations by varying photo-z parameters. For each set of parameters, we fix bias at the lowest chi square value.
- For the combined bin case, we also further consider the bias redshift evolution, approximated via quadratic curve.
- The galaxy biases (and the evolution) are fixed for the CMB cross-correlation analysis.

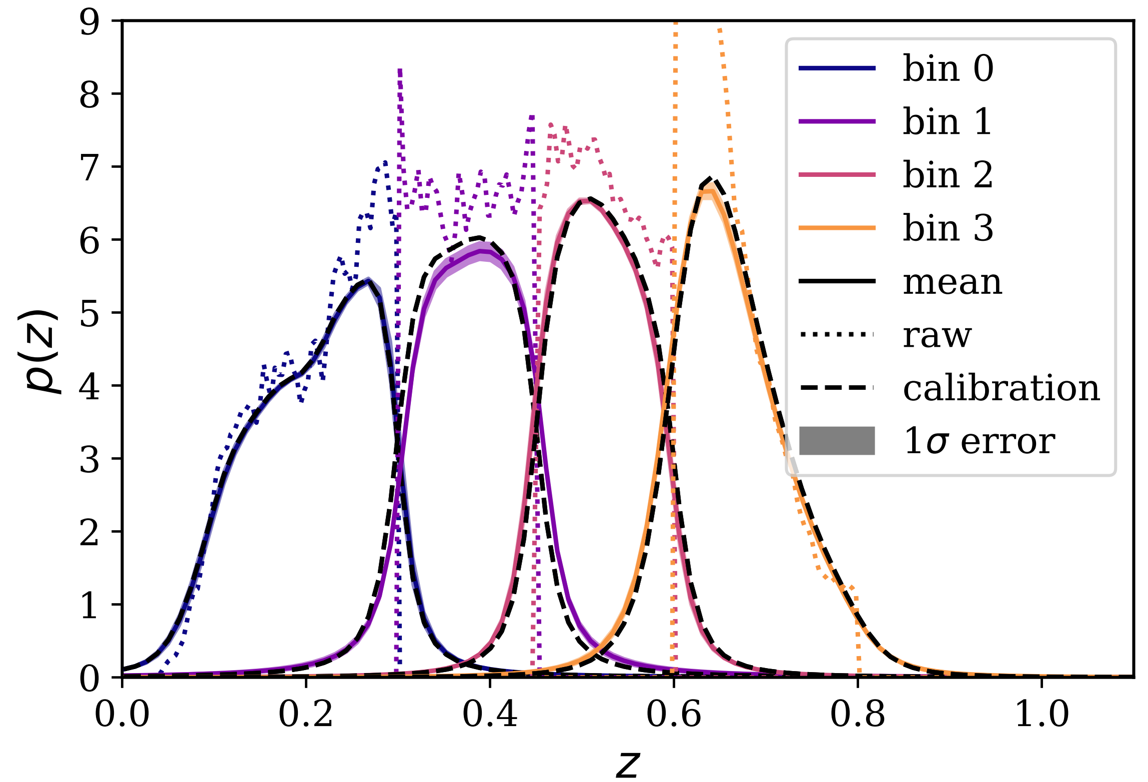

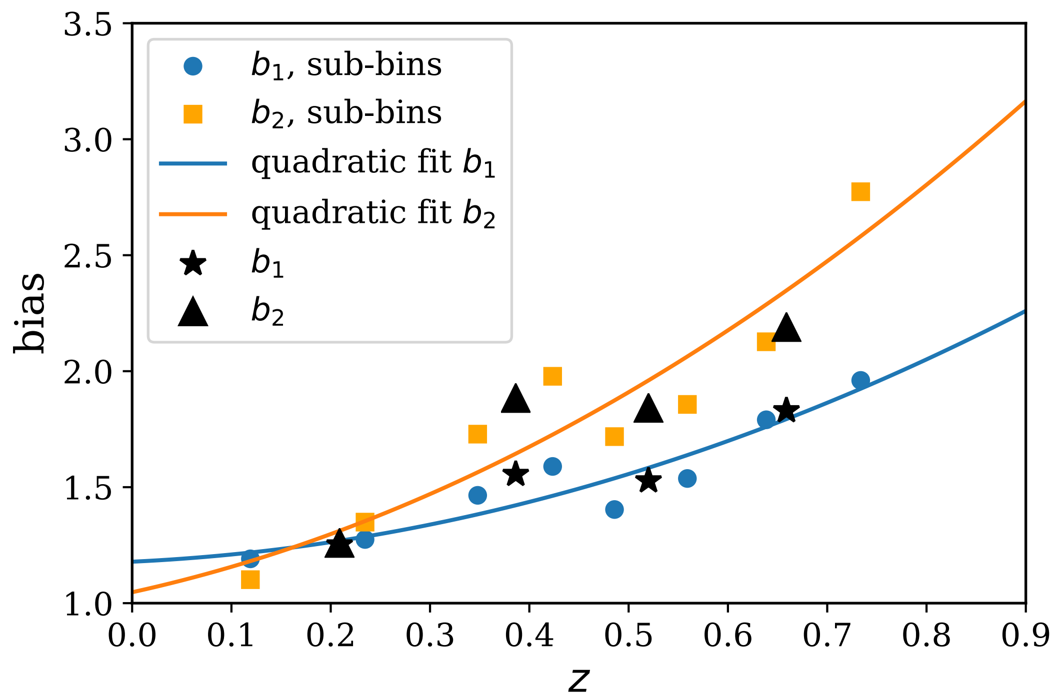

Cosmological implications of low A_κ

There are also implications on the H_0 tension…

Since the acoustic scale mainly fixes $\Omega_m h^3$, a lower Ω_m needs higher h.

Our preferred Ω_m=0.27 would yield h=0.71, consistent with the local universe measurements from e.g., distance ladder.

For more info: Q. Hang et al 2020, arXiv: 2010.00466

My other ongoing works:

Stacking of super structures in the Legacy Survey with CMB [Q. Hang et al. in prep.]

RSD from group-galaxy cross-correlation using GAMA [Q. Hang et al. in prep.]

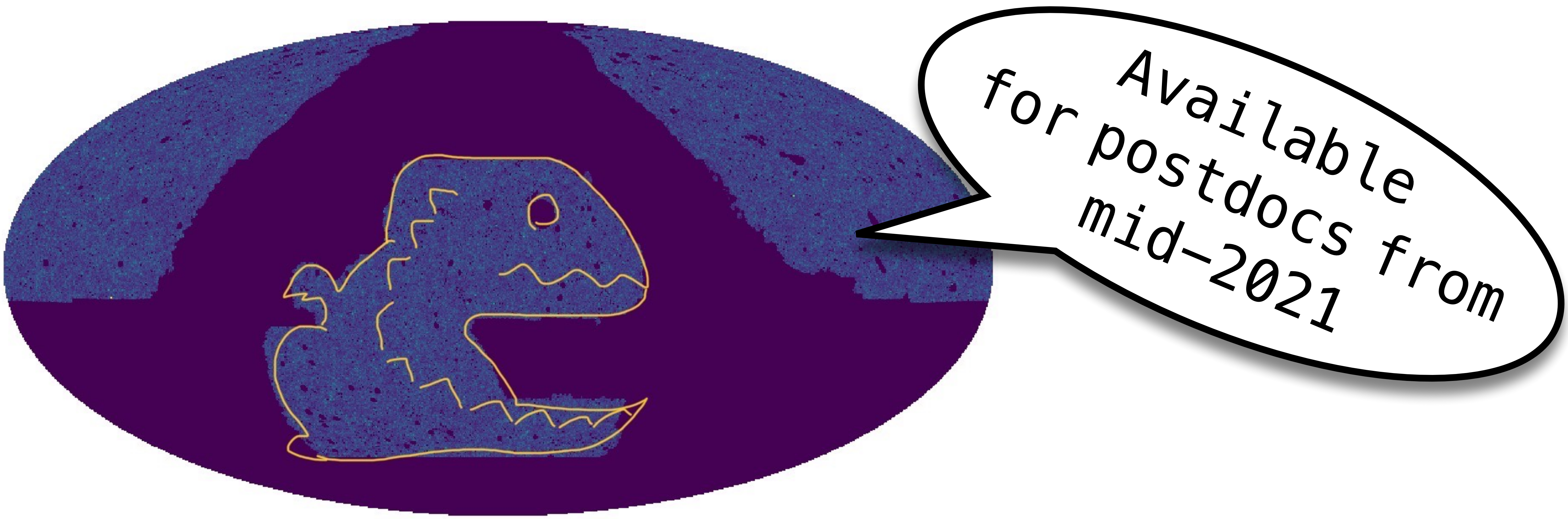

Modelling the signal

$$\frac{\ell(\ell+1)}{2\pi} C_\ell^{gX} = \frac{\pi}{\ell} \int b\, \Delta^2(k=\ell/r, z)\, p(z) K^X(z) r\, dz$$

galaxy bias

matter power spectrum

redshift distribution

X=Lensing $$K^\kappa = \frac{3H_0^2\Omega_m}{2c^2 a} \frac{r(r_{\rm LS}-r)}{r_{\rm LS}}$$

X=ISW Assume linear theory, $$\Phi = \frac{3H_0^2\Omega_m}{2ak^2}\delta$$

$$K^T = \frac{2T_{\rm CMB}}{c^3} \frac{3H_0^2\Omega_m}{2k^2} H(z)\,(1-f_g(z))$$

growth rate

Theory: galaxy-galaxy auto/ cross-correlations

Galaxy bias and redshift distribution can be constrained from the galaxy-galaxy correlations, given fixed cosmology.

$$\frac{\ell(\ell+1)}{2\pi}C_\ell^{gg} = \frac{\pi}{\ell}\int b_1 b_2\,\Delta^2(k=\ell/r,z)\,p_1(z)p_2(z)\frac{H(z)r}{c}dz$$

In principle, the galaxy bias can have redshift and scale dependence.

p1=p2 -> auto-correlation,
p1≠p2 -> cross-correlation between different redshift slices.

Density map systematic correction

Mean density split in bins of stellar number and E(B-V)

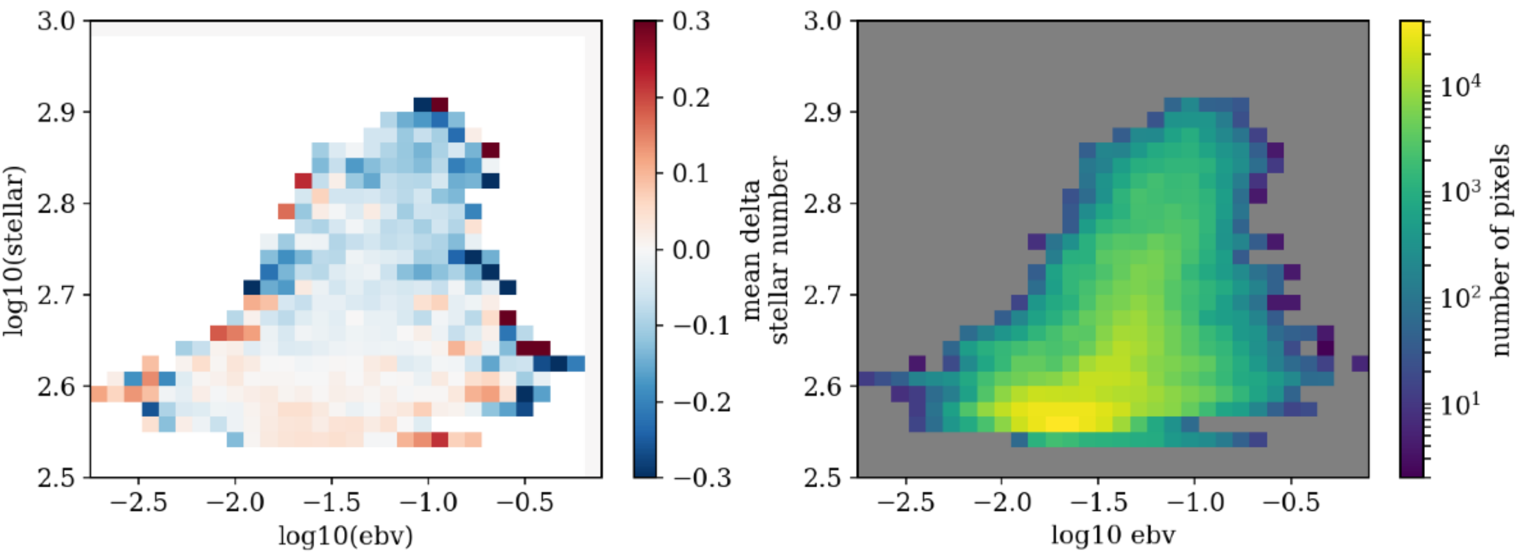

Density variation with stellar density

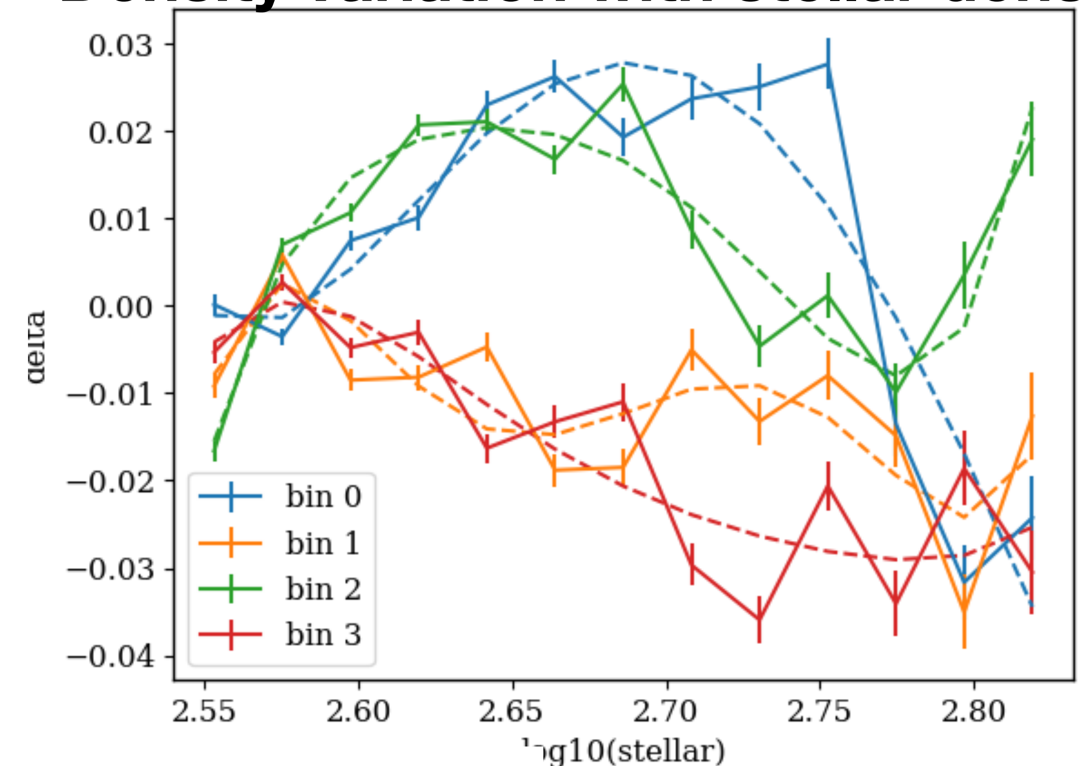

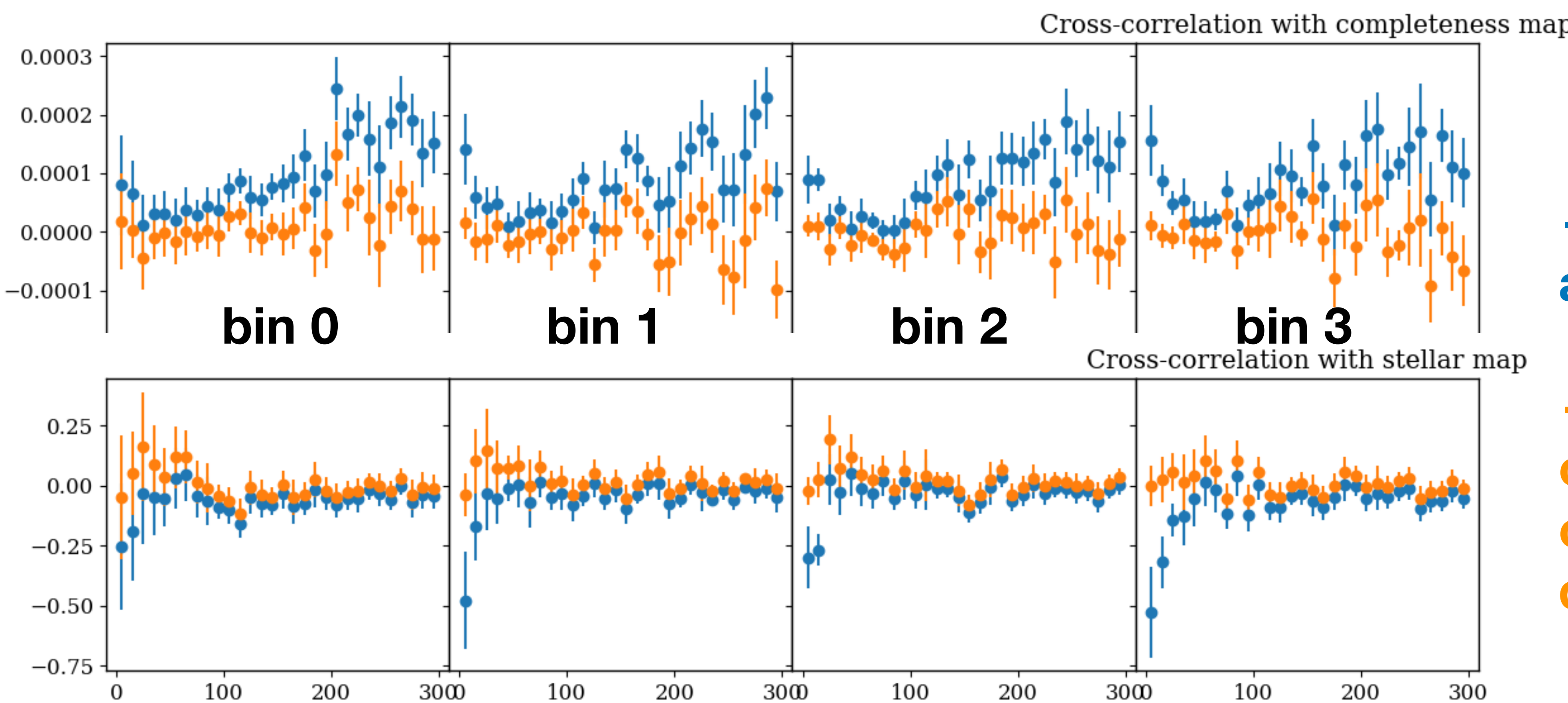

— Before weighting and stellar correction

— Weighted by completeness and corrected by stellar density

Mask, shotnoise, errorbars

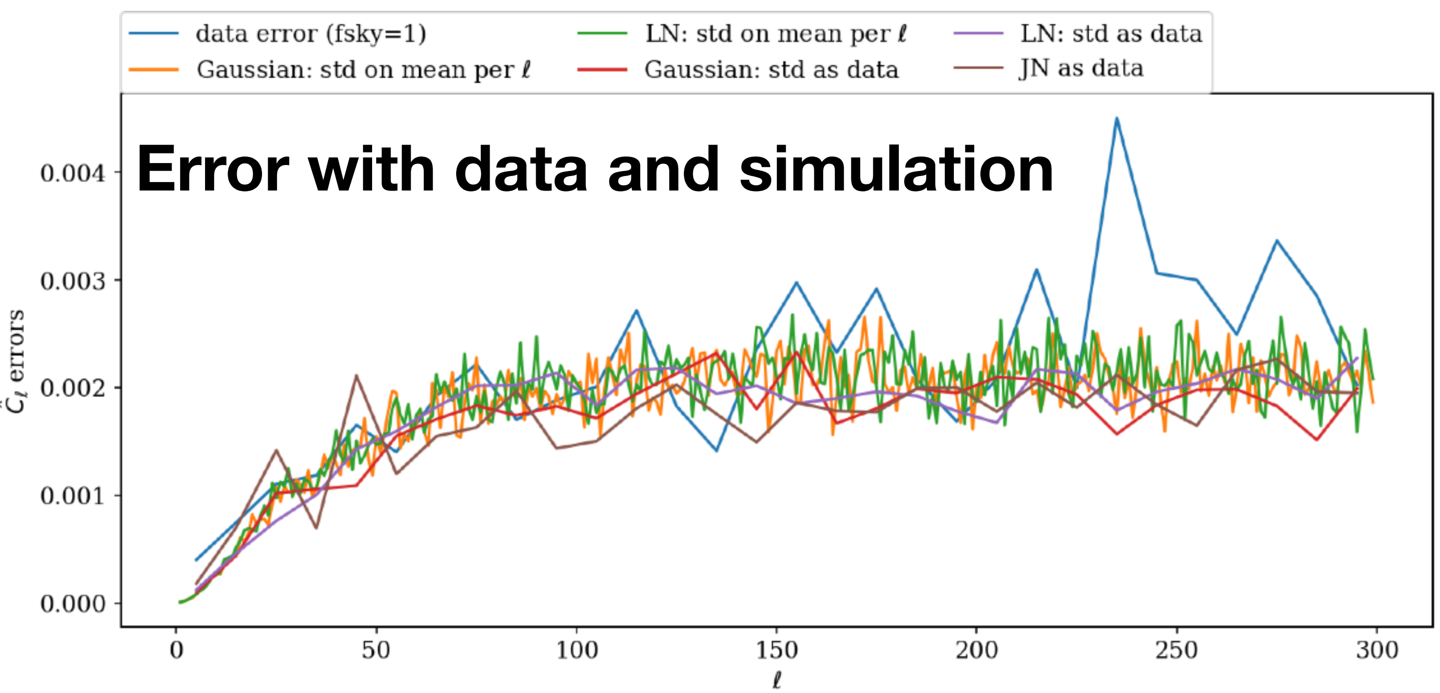

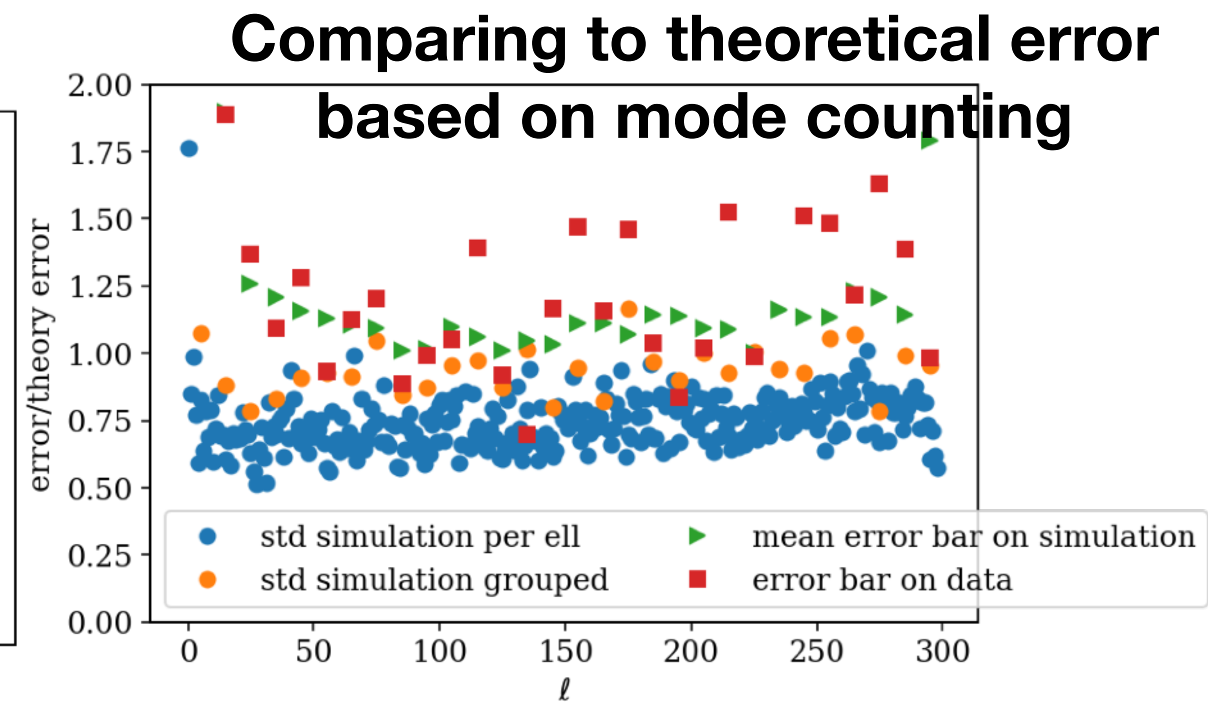

Including mask and shot noise

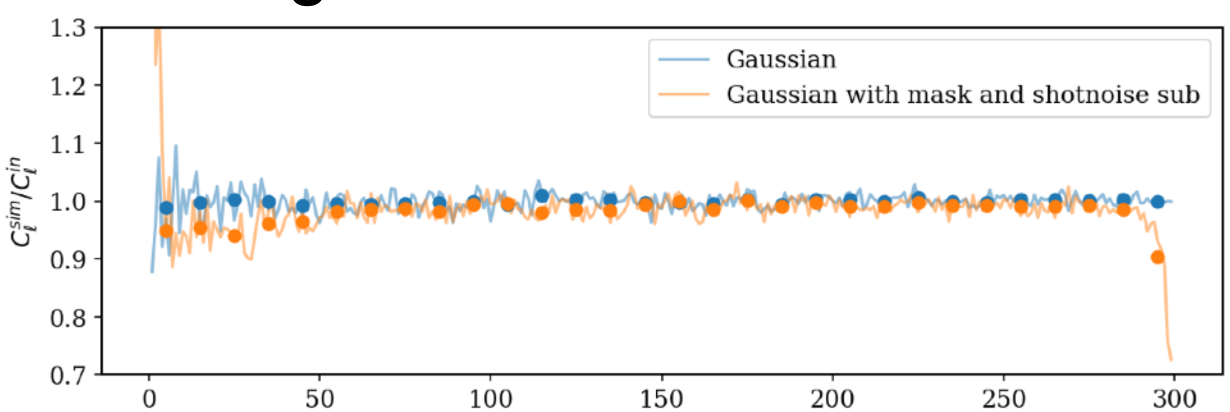

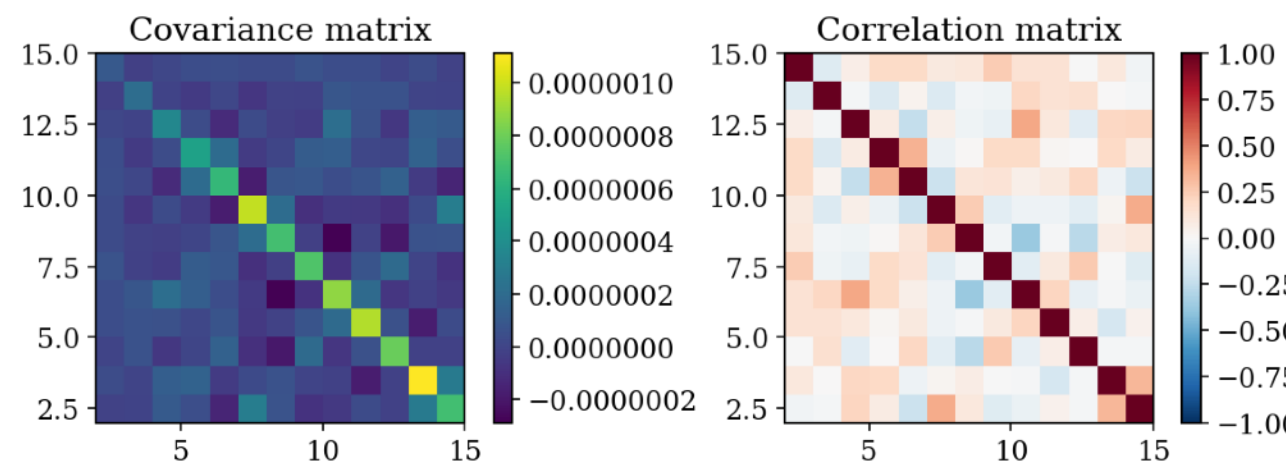

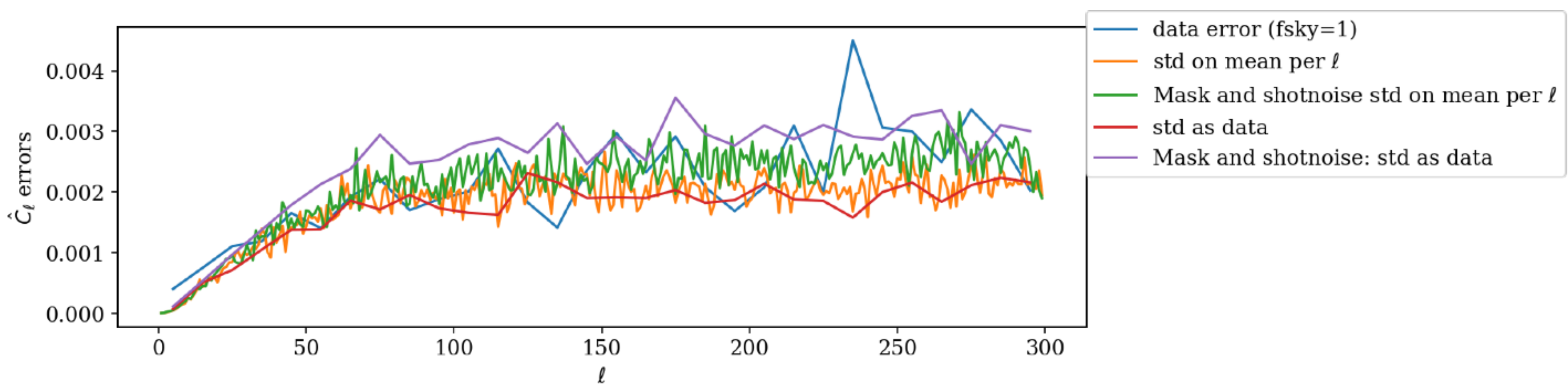

Covariance from 50 simulations for modes between 10<l<150, with mask and shot noise.

2–bias model

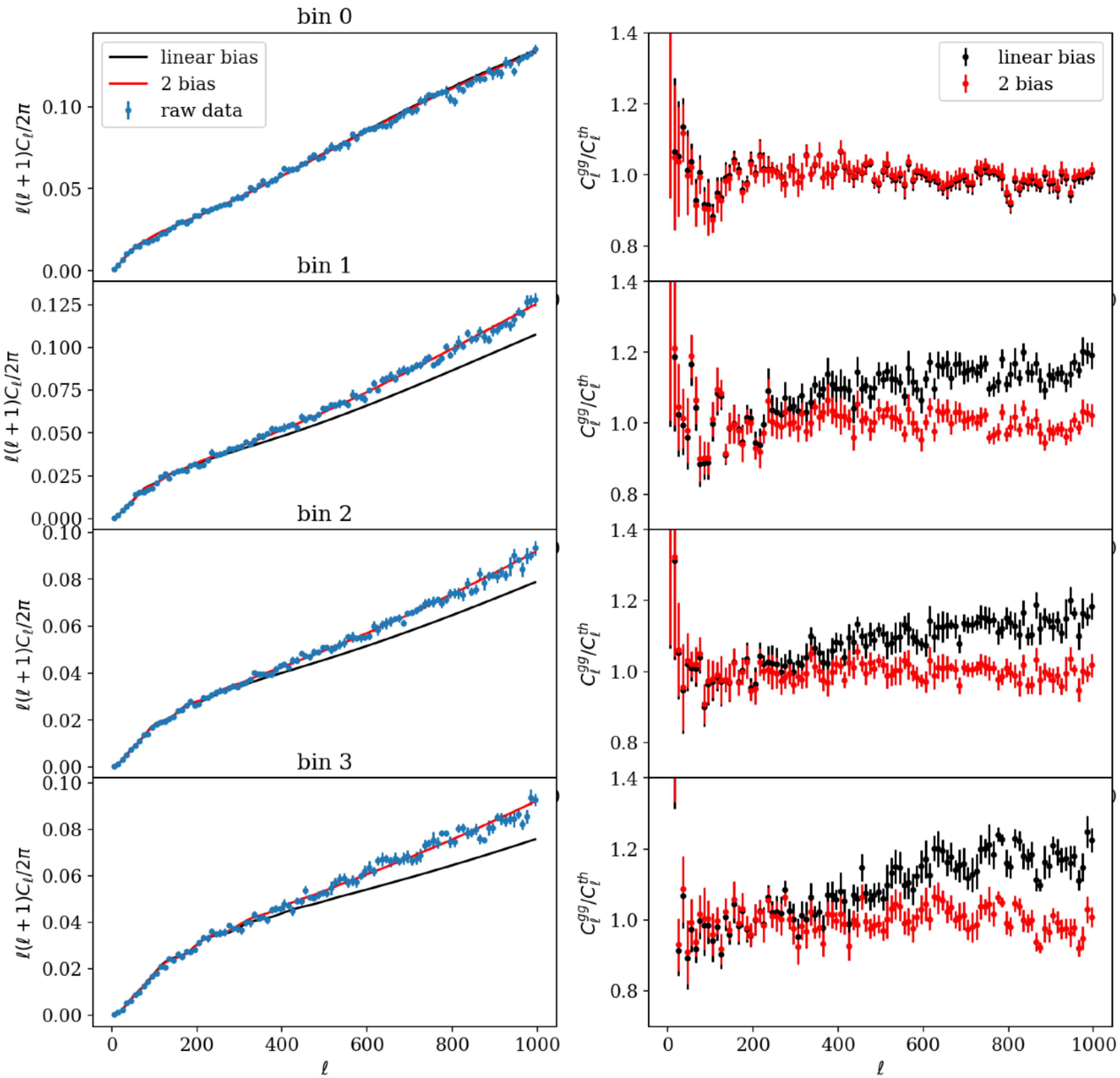

The ratio between data and model with a constant bias show a change at transition between linear and non-linear scales. The ratio on either end of the scales seem flat.

Comparison between our photo-z and [Zhou et. al. 2020]

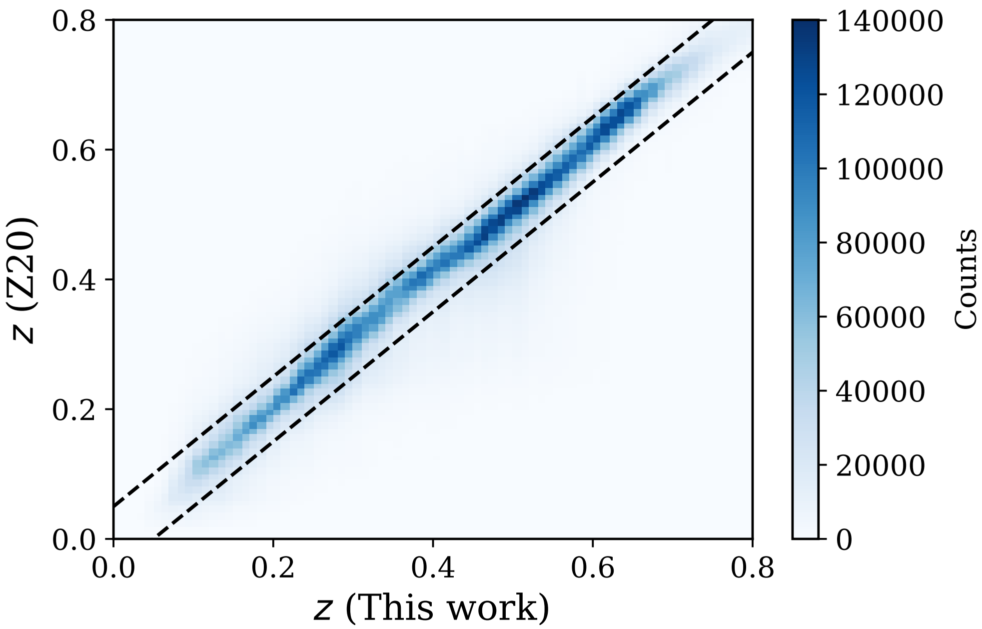

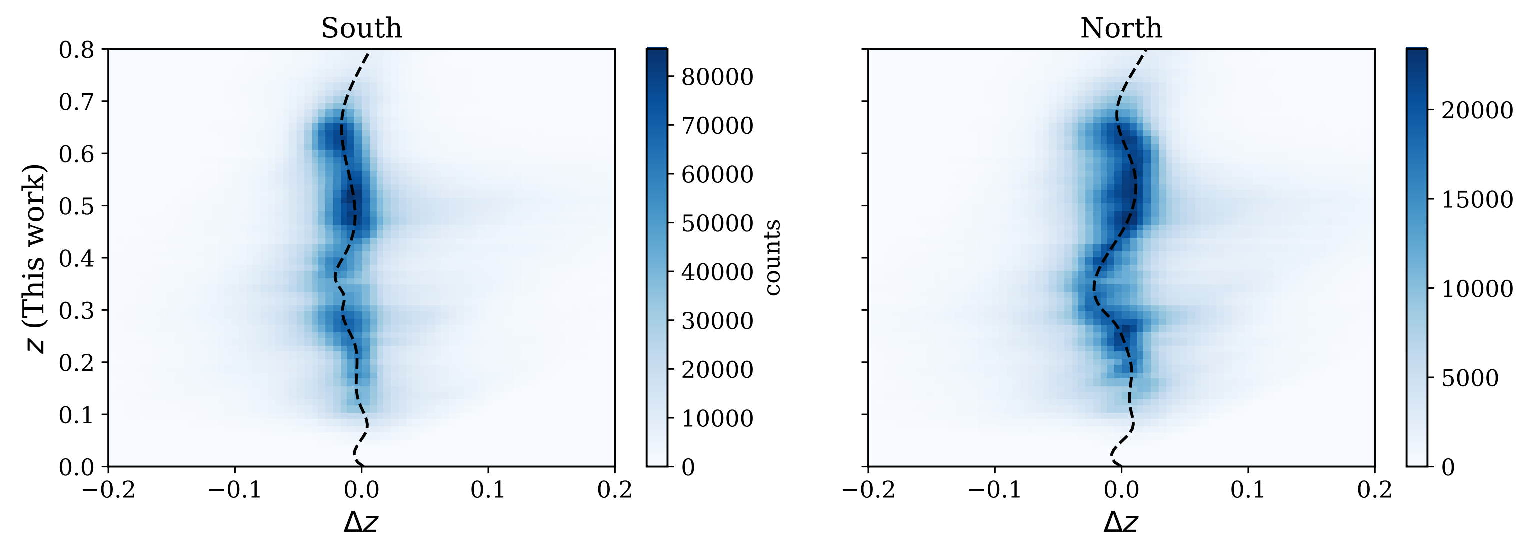

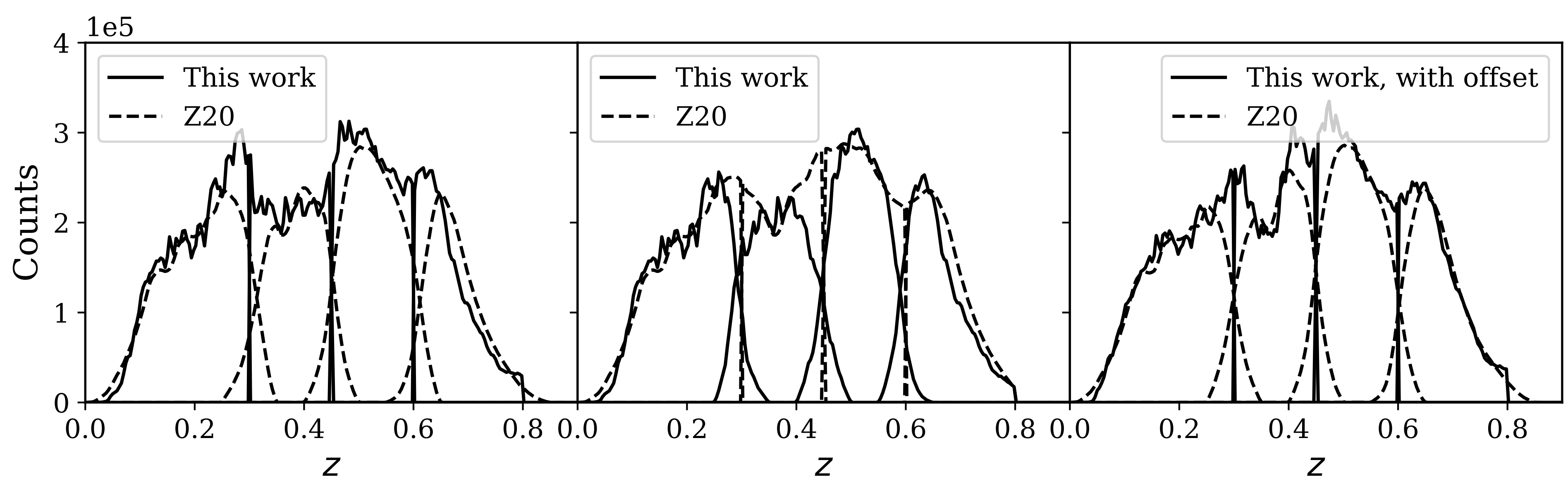

Systematic tests

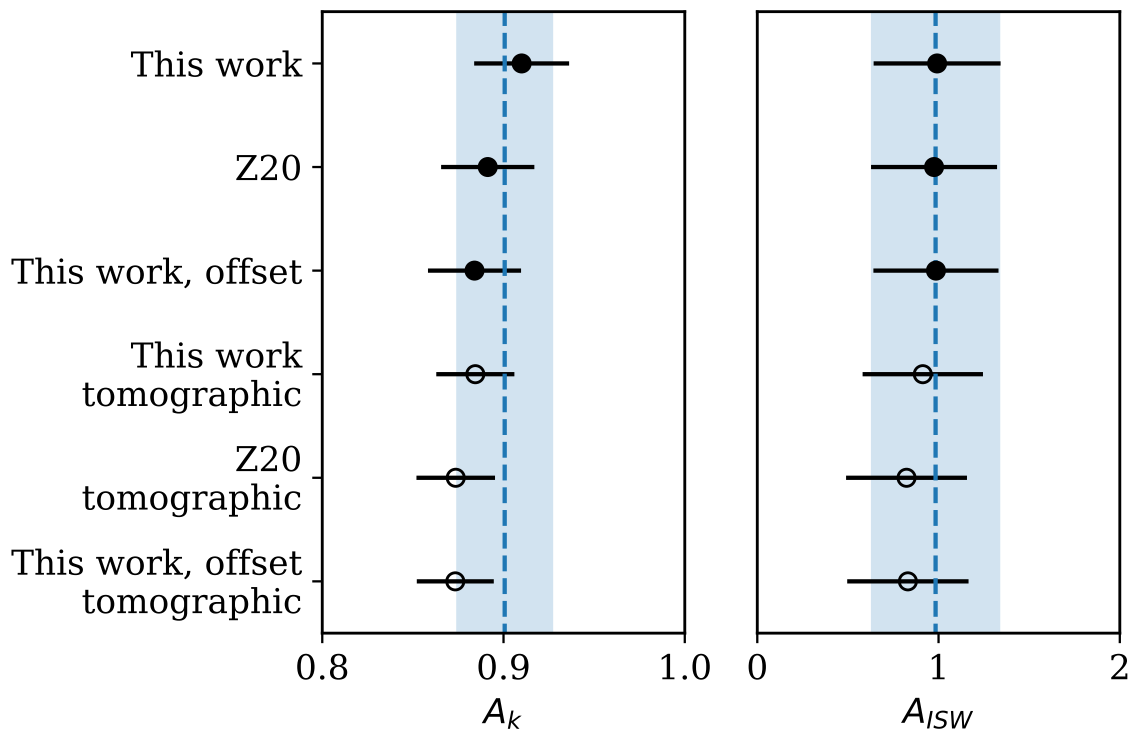

Parameters	bin0	bin1	bin2	bin3	combined	Un-binned
Redshift	$0 < z \leq 0.3$	$0.3 < z \leq 0.45$	$0.45 < z \leq 0.6$	$0.6 < z \leq 0.8$	-	$0 < z \leq 0.8$
Marginalized over $p(z)$						
b_1	1.25 ± 0.01	1.53 ± 0.02	1.54 ± 0.01	1.86 ± 0.02	-	-
b_2	1.27 ± 0.01	1.85 ± 0.03	1.82 ± 0.01	2.23 ± 0.02	-	-
A_k	0.91 ± 0.05	0.82 ± 0.04	0.94 ± 0.04	0.90 ± 0.04	0.89 ± 0.02	-
$A_{\rm ISW}$	0.52 ± 0.78	1.20 ± 0.63	1.48 ± 0.61	0.18 ± 0.67	0.91 ± 0.33	-
Best-fit $p(z)$						
b_1	1.25	1.56	1.53	1.83	-	1.43
b_2	1.26	1.88	1.84	2.19	-	1.59
A_k	0.91 ± 0.05	0.80 ± 0.04	0.94 ± 0.04	0.91 ± 0.04	0.88 ± 0.02	0.91 ± 0.03
$A_{\rm ISW}$	0.52 ± 0.75	1.17 ± 0.58	1.44 ± 0.52	0.18 ± 0.67	0.91 ± 0.33	0.99 ± 0.35
Zhou et. al.						
b_1	1.25	1.54	1.55	1.90	-	1.44
b_2	1.26	1.87	1.90	2.21	-	1.62
A_k	0.91 ± 0.06	0.81 ± 0.04	0.93 ± 0.04	0.87 ± 0.04	0.87 ± 0.02	0.89 ± 0.03
$A_{\rm ISW}$	0.50 ± 0.79	1.03 ± 0.59	1.37 ± 0.55	0.20 ± 0.63	0.82 ± 0.33	0.98 ± 0.35
Offset						
b_1	1.28	1.52	1.54	1.89	-	1.45
b_2	1.30	1.86	1.87	2.20	-	1.64
A_k	0.89 ± 0.05	0.81 ± 0.04	0.93 ± 0.04	0.89 ± 0.04	0.87 ± 0.02	0.88 ± 0.03
$A_{\rm ISW}$	0.45 ± 0.81	1.05 ± 0.58	1.32 ± 0.56	0.25 ± 0.46	0.83 ± 0.33	0.99 ± 0.35
AvERA model						
b_1	1.16	1.34	1.25	1.46	-	1.23
b_2	1.11	1.50	1.45	1.75	-	1.33
A_k	0.97 ± 0.06	0.80 ± 0.04	0.91 ± 0.04	0.85 ± 0.04	0.87 ± 0.02	0.91 ± 0.03
$A_{\rm ISW}$	0.24 ± 0.35	0.48 ± 0.25	0.55 ± 0.23	0.07 ± 0.24	0.35 ± 0.13	0.39 ± 0.14